POLARIZED MONOLAYERS FORMED BY EPITHELIAL CELLS ON A PERMEABLE AND TRANSLUCENT SUPPORT

M. CEREIJIDO, E. S. ROBBINS, W. J. DOLAN, C. A. ROTUNNO, and D. D. SABATINI

From the Department of Cell Biology, New York University Medical Center, New York 10016, el Centro de Investigaciones y Estudios Avanzados del Instituto Politecnico Nacional, Apartado Postal 14-740, Mexico, and The Borough of Manhattan Community College, The City University of New York, New York 10019

ABSTRACT

An epithelial cell line (MDCK) was used to prepare monolayers which, in vitro, develop properties of transporting epithelia. Monolayers were formed by plating cells at high densities (10^6 cells/cm^2) on collagen-coated nylon cloth disks to saturate the area available for attachment, thus avoiding the need for cell division.

An electrical resistance developed within 4–6 h after plating and achieved a steady-state value of 104 ± 1.8 $\Omega \cdot cm^2$ after 24 h. Mature monolayers were morphologically and functionally polarized. They contained junctional complexes composed of desmosomes and tight junctions with properties similar to those of "leaky" epithelia. Monolayers were capable of maintaining a spontaneous electrical potential sensitive to amiloride, produced a net water flux from the apical to basal side, and discriminated between Na^+ and Cl^- ions.

The MDCK permeability barrier behaves as a "thin" membrane with negatively charged sites. It has: (*a*) a linear conductance/concentration relationship; (*b*) an asymmetric instantaneous current/voltage relationship; (*c*) a reduced ability to discriminate between Na^+ and Cl^- caused by lowering the pH; and (*d*) a characteristic pattern of ionic selectivity which suggests that the negatively charged sites are highly hydrated and of medium field strength.

Measurements of Na^+ permeability by electrical and tracer methods ruled out exchange diffusion as a mechanism for ion permeation and the lack of current saturation in the $I/\Delta\Psi$ curves does not support the involvement of carriers. The discrimination between Na^+ and Cl^- was severely but reversibly decreased at low pH, suggesting that Na^+-specific channels which exclude Cl^- contain acidic groups dissociated at neutral pH.

Bound Ca^{++} ions are involved in maintaining the integrity of the junctions in MDCK monolayers as was shown by a reversible drop of resistance and opening of the junctions in Ca^{++}-free medium containing EGTA.

Several other epithelial cell lines are capable of developing a significant resistance under the conditions used to obtain MDCK monolayers.

KEY WORDS epithelial monolayers · polarized cells · plasma membrane · junctional complexes · transporting epithelia

Cells of transporting epithelia form layers which act as permeability barriers between physiological compartments. An understanding of the function of transporting epithelia has been advanced considerably by the introduction of model systems, such as the frog skin (47), gallbladder (27), and intestinal mucosa (71), to study permeability and electrical properties in vitro. Thus, much information has been obtained which serves to explain some of the overall physiological characteristics of epithelia and their role in the production of fluids and absorbates. More recently, it has become possible to attempt an interpretation of the function of epithelia in terms of cellular features and the molecular mechanisms involved in transport and permeability. It is now apparent that the extent to which transepithelial fluxes follow a passive paracellular pathway through the transcellular route is determined by junctional complexes between the cells (35). In addition, vectorial transport of ions and small molecules across the epithelial cell cytoplasm requires that opposite sides of the plasma membranes (i.e., luminal and basolateral aspects) be endowed with different specialized biochemical properties.

To understand the mechanisms which lead to the functional specialization of selected regions of the cell membrane and, in particular, to the formation of junctional complexes in epithelia, we have studied an in vitro preparation of cultured cells of renal origin. The MDCK cell line introduced by Madin and Darby (54) was chosen for this work because of the observations of Leighton and his colleagues (50, 51, 1) demonstrating that, under appropriate conditions, these cells form monolayers which develop many of the properties normally found in natural epithelia-including a unidirectional transport of water. During the course of this investigation, Misfeldt et al. (59) presented a study of MDCK monolayers grown on Millipore filters (Millipore Corp., Bedford, Mass.), demonstrating that these monolayers constitute an effective permeability barrier with morphological and functional properties of transporting epithelia. Several of the findings reported here (using a different technique to form the monolayers) confirm, complement, and extend their observations.

This paper describes a procedure for preparing MDCK monolayers by plating the cells at high densities on a permeable and translucent support which can be mounted as a flat sheet between two bathing solutions. A study of the organization and permeability of MDCK monolayers is also presented, demonstrating that they are structurally and functionally polarized with properties similar to those of natural "leaky epithelia" such as kidney proximal tubules (38, 9), intestinal mucosa (36, 71), gallbladder (61), and choroid plexus (85), which have an important paracellular permeation route controlled by tight junctions. The physiological role of natural leaky epithelia serves to underline the usefulness of developing and characterizing semiartificial preparations like the one employed here, in which a number of important parameters can be controlled experimentally.

MATERIALS AND METHODS

Cell Culture

Starter MDCK cultures were obtained from the American Type Culture Collection (MDCK, CCL-34) (54) or were generously provided by Prof. J. Leighton (Department of Pathology, University of Pennsylvania, Philadelphia, Pa.). The latter cells were used in most of the experiments discussed here. Other cell lines obtained from the American Type Culture Collection are: BHK-21, CCL-10 (baby hamster kidney); BS-C-1, CCL-26 (African green monkey kidney); and SIRC, CCL-60 (normal rabbit cornea). Human fetal lung fibroblasts (WI-38) were obtained from Dr. L. Hayflick, and MDBK (bovine kidney) cells were a gift of Dr. M. Krug and Dr. P. R. Etkind (Memorial Sloan-Kettering Cancer Center, New York).

Cells were grown at 36.5°C in roller bottles with an air-5% CO_2 atmosphere and 100 ml of Complete Eagle's Minimal Essential Medium (CMEM) with Earle's salts (Grand Island Biological Co. [GIBCO] F-11, Grand Island, N. Y.), 100 U/ml of penicillin, 100 μg/ml of streptomycin, 0.5 μg/ml of Fungizone (E. R. Squibb & Sons, Inc., New York), and 30% calf serum (GIBCO 617). Cells were harvested with trypsin-EDTA (GIBCO 540), and counted in a chamber with Neubauer rulings. Trypan blue dye exclusion tests indicated a viability >95%. Tests for *Mycoplasma* were conducted according to the technique of Chen (22) and the cells were found to be *Mycoplasma*-free.

Preparation of the Permeable and Translucent Support

Disks (1–1.4 cm in diameter) of nylon cloth with 103-μm square mesh openings (HC-103 Nitex; Tetko, Inc., Elmsford, N. Y.) were cleaned by sonication in acetone (5–10 min) and placed for 5–10 min in boiling distilled

water. They were passed through a series of alcohols of increasing concentrations and air-dried before coating with collagen. Collagen was prepared by a modification of the method of Bornstein (8). Briefly stated, rat tail tendons were dissected, rinsed in a normal saline solution, minced with scissors, and dissolved in 2% acetic acid at 4°C. The collagen solution was centrifuged at 2,000 *g* for 1 h at 4°C to remove insoluble material, and the supernate was dialyzed extensively against distilled water at 4°C. Disks were briefly immersed into the collagen solution (5–10 mg/ml) at 0–4°C, exposed at room temperature to ammonia fumes for 2–5 min, and placed in a 4% solution of glutaraldehyde for 1–3 h to promote cross-linking. After thorough washing in several changes of sterile normal saline solution, disks were sterilized by exposure to UV light for 1.5–3 h and stored at 4°C in saline until needed. A low-power scanning electron micrograph of a collagen-coated disk is shown in Fig. 1. These disks are permeable, flexible, and translucent. This facilitates the handling and mounting of the preparation for electrical studies and measurements of fluxes. Because disks are translucent, formation of a cell monolayer may be followed by phase microscopy to determine its completeness before use. Occasional squares of mesh not covered by collagen or cells are easily recognized at low magnification.

Preparation of the Cell Layer

Each disk was placed into a 16-mm diameter well of a multichamber dish (Linbro Chemical Co., New Haven, Conn.), and a suspension of MDCK cells in CMEM was added to a density of 10^6 cells/cm^2. After incubation for 90 min at 36.5°C in an air-5% CO_2 atmosphere with constant humidity to allow for attachment of the cells, disks were transferred to individual Petri dishes (35 mm in diameter) or to other multidish chambers containing fresh CMEM.

Electrical Tests

The disk was mounted as a flat sheet between two (5.0 ml each) Lucite chambers. Exposed areas varied from 0.2 to 0.9 cm^2. The electrical potential difference between the two chambers was measured with agar-salt bridges placed 1.0 mm from each side of the disks, or with Ag/AgCl electrodes which were connected to a Keithley 600B electrometer (Keithley Instruments, Inc., Cleveland, Ohio). All measurements were corrected for junction potentials at the tips of the salt bridges, or for potentials between the two Ag/AgCl electrodes when solutions of different chloride activities were used.

In experiments in which both chambers contained the same solution, the suitability of the Ag/AgCl electrodes was checked routinely by immersing both in a single chamber at the same distance from each other as when in their normal positions. Electrode pairs with more than 0.2 mV between their tips were discarded.

In experiments in which different solutions were used on each side of the membrane, electrodes were controlled in the following manner: two to three Millipore filters were mounted between the two chambers which were filled with the desired solutions. The voltage measured was compared with the value obtained by adding that calculated on the basis of the Nernst equation to the diffusion potential (E) between the two solutions calculated as follows:

$$E = \frac{RT}{F}(T_+ - t_-)\ln\frac{a''}{a'},$$

where F is the Faraday constant, a'' and a' are the activities of the two sides, and t_+ and t_- are the transference numbers for the major cation and anion, respectively.

Electrical tests seldom lasted >2 h, and were conducted under clean but not sterile conditions. The poten-

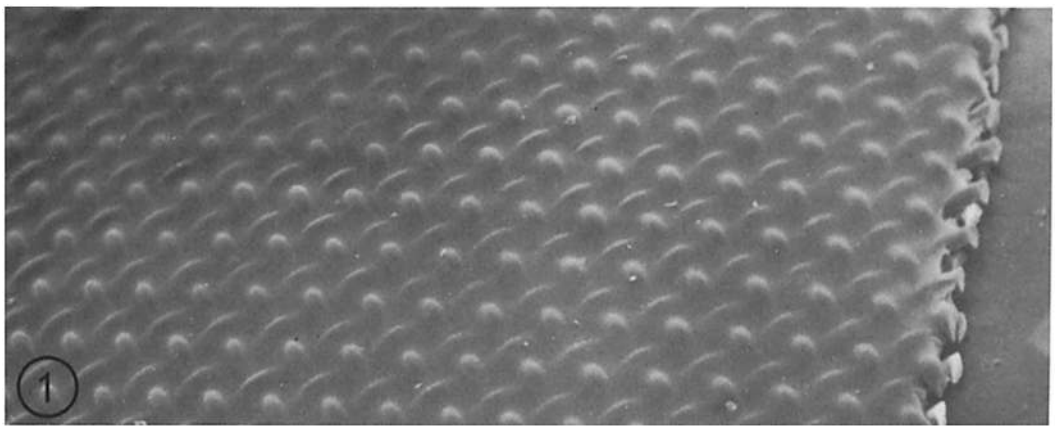

FIGURE 1 Scanning electron micrograph of a collagen-coated nylon cloth disk. Note that the smooth collagen layer is continuous and follows the contours of the fibers of the cloth. This particular disk had a complete cell monolayer on the obverse side. × 27.6.

tial difference between electrodes (E) was calculated as follows:

$$E = (RT/F) \ln (a^i_{Cl}/a^o_{Cl}) \quad (1)$$

where (a^i_{Cl}/a^o_{Cl}) is the chloride activity ratio as calculated from the concentrations and the activity coefficients listed in reference 67. The electrical conductance was measured by recording with a Simpson (Simpson Electric Co., Elgin, Ill.) or a Keithly 600C microammeter the amount of current delivered by two Ag/AgCl electrodes necessary to produce a change of 10 mV in electrical potential. The contribution of a collagen-coated nylon disk without cells was subtracted from all calculated values of resistance. Measurements were performed either in CMEM without penicillin, Fungizone, or streptomycin, or in a saline solution containing: 150 mM NaCl, 0.25 mM $CaCl_2$, and 1.5 mM tris buffer at pH 7.4.

Net Water Flux

A modification of the method of Bourguet and Jard (11) was used. A monolayer on a collagen-coated nylon disk with an exposed area of 0.64 cm^2 was mounted between two chambers. Net water fluxes at 22°C were measured automatically by recording the amount of fluid which had to be added or subtracted to the inner chamber (i.e., on the collagen side) to maintain its volume constant.

Specific Ion Conductances

The conductances were determined in monolayers mounted between two Lucite chambers containing Ringer's solutions with LiCl, NaCl, KCl, RbCl, or CsCl as the main salt (150 mM in each case) without addition of antibiotics or Fungizone. Areas of monolayers exposed in the chamber were either 0.1 or 0.2 cm^2. The amount of current necessary to produce a fixed voltage change (10 or 30 mV) was determined. Voltage was measured with a pair of Ag/AgCl electrodes connected to a high input impedance electrometer (Keithley, model 600B). All measurements were corrected for potentials (E) between the electrodes when solutions of different chloride activities were used. These potentials were computed using the chloride activity ratio: $E = (RT/F) \ln (a^o_{Cl}/a^i_{Cl})$. The value of the conductance was corrected for the conductance of the solutions between the tips of the electrodes with an empty collagen-coated nylon disk in place. When the selectivity to cations was studied, each measurement of conductance in a given salt solution was preceded and followed by a measurement of the conductance in NaCl-Ringer's solution. Changes in solutions were made simultaneously on both sides to eliminate hydrostatic effects. Three washes with the new solutions were made immediately, and a fourth one was made several minutes later just before the determination of the conductance. Specific ion conductances for Na^+ and Cl^- were calculated from the values of the total conductances and the ratio (β) of the chloride (P_{Cl}) and sodium (P_{Na}) permeabilities. This ratio, ($\beta = P_{Cl}/P_{Na}$), was obtained through the well-known Goldman-Hodgkin-Katz equation using the dilution potential measured in membranes mounted between a 2:1 concentration gradient of NaCl (with the osmolarity maintained with mannitol).

Instantaneous Current/Voltage Relationships

Chambers similar to those described above (exposed area: 0.11 cm^2) were used. Conventional techniques for recording electrical potentials and for passing current were employed. The potential was differentially measured across the monolayer with a high impedance differential amplifier. Inputs were delivered from an isolation unit which was triggered by a Tektronix series 160 wave form generator (Tektronix, Inc., Beaverton, Ore.). One of the current electrodes was connected to one output of the isolation unit via a 1.00 ± 0.1- and a 100-kΩ resistor in series. The other current electrode was directly connected to the second output of the isolation unit which was grounded. The current was measured as a voltage drop across the 1-kΩ resistor. Voltage and current signals were displayed on a Tektronix K-13 dual beam oscilloscope with storage, equipped with a camera (Polaroid Corp., Cambridge, Mass.). All measurements were corrected for values obtained under the same conditions with a collagen-coated disk without a monolayer.

Sodium Fluxes

Different Lucite chambers were used, ranging in window area from 0.2 to 7.97 cm^2 and in volume of each side from 2.0 to 8.0 ml. The electrical resistance was monitored frequently. 1 μCi of ^{22}Na was added to the inner bathing solution which behaved as an infinite reservoir. After allowing 10 min for equilibration, 500-μl samples were taken from the opposite chamber every 10 min. The volume removed was replaced with fresh solution containing no tracer. Three to five samples of the inner solution were taken at 10-min intervals. ^{22}Na radioactivity was measured in a well-type scintillation counter (Nuclear-Chicago Corp., Des Plaines, Ill.) set as a spectrometer in the ^{22}Na peak. The flux of ^{22}Na is expressed as micromoles per hour per square centimeter.

Transmission Electron Microscopy

Monolayers on disks or plastic Petri dishes were fixed with cold 2% glutaraldehyde in 0.1 M sodium cacodylate buffer (68) with or without 0.1 M sucrose (6) for 1–3 h. After three buffer rinses, samples were postfixed in 2% OsO_4 in the buffer described above. Samples were block-stained with 1% aqueous uranyl acetate, dehydrated in a graded ethanol series, and embedded in Epon 812. 0.5-μm thick sections, cut on glass knives, were stained with aqueous 1% toluidine blue. Thin sections were cut with diamond knives, picked up on parlodion-coated,

carbon-stabilized copper grids, stained with lead citrate and uranyl acetate, and examined in a Siemens 1A or Philips 301 electron microscope.

Electron Microscope Tracers

Lactoperoxidase (50 U/mg per ml) in distilled water was applied to monolayers on disks which had been previously fixed in glutaraldehyde for 45 min, rinsed in buffer, and supported on a wax plate with a Teflon ring of a slightly smaller diameter clamped onto the upper surface to create a small well. After 30 min, the disk with Teflon ring in place was rinsed three times with distilled water, treated with diaminobenzidine (DAB) for 15 min (48) and rinsed with tris buffer and distilled water. Disks were then processed as described above.

The same Teflon ring technique was used to apply 1% lanthanum in 2% glutaraldehyde to the upper or lower surfaces of unfixed disks. Lanthanum was present in all subsequent solutions used for processing the disks for Epon embedding, including absolute ethanol (66).

Scanning Electron Microscopy

Cell monolayers were fixed and dehydrated as for embedding. Critical-point drying from absolute ethanol into liquid CO_2 was carried out in a Bomar apparatus (Bomar Co., Tacoma, Wash.) without employing a transition fluid (23). Dried specimens affixed to aluminum stubs with double-sided tape were coated in an evaporator (Denton Vacuum Inc., Cherry Hill, N. J.), first with carbon, then with gold and palladium (60 and 40%, respectively). Specimens were examined in an AMR 1000 scanning electron microscope at 20 kV.

Freeze-Fracture

Confluent monolayers obtained after heavy plating on plastic Petri dishes were fixed *in situ* with cold 2% glutaraldehyde in 0.1 M sodium cacodylate buffer for 1 h. Monolayers were scraped off with a Teflon spatula in 0.1 M buffer, and fragments were recovered by sedimentation. After three buffer rinses, the cells were infiltrated with 20% glycerol in 0.1 M sodium cacodylate for at least 1 h. Freezing was done in Freon 22 (E. I. du Pont de Nemours & Co., Wilmington, Del.) cooled by liquid nitrogen. Samples were fractured at −120°C and 4×10^{-6} torr in a Balzers apparatus (Balzers High Vacuum Corp., Santa Ana, Calif.), and carbon-platinum replicas supported by a carbon film were prepared employing a crystal thin film monitor. Replicas were cleaned with commercial bleach, picked up from distilled water onto either 300-mesh uncoated grids or 200-mesh parlodion- and carbon-coated grids.

Sources of Materials

Amiloride (3,5-diamino-6-chloropyrazinoylguanidine hydrochloride) was purchased from Merck Sharp & Dohme Div., West Point, Pa.; ethylene glycol-bis(β-amino-ethyl ether)-*N,N*-tetraacetic acid (EGTA) from Sigma Chemical Co., St. Louis, Mo.; potassium penicillin G and Fungizone (amphotericin B) from E. R. Squibb & Sons; streptomycin sulfate from Pfizer Chemicals Div., New York; and lactoperoxidase from Calbiochem, San Diego, Calif. Ca^{++}-free Eagle's Minimal Essential Medium (MEM) was prepared from 50X MEM amino acids and 100X MEM vitamins (GIBCO) plus reagent-grade individual salts of the MEM medium except Ca^{++}. Ca^{++} concentration was estimated to be 2×10^{-5} M. The 10% fetal calf serum used was dialyzed against Ca^{++}-free phosphate-buffered saline (PBS) (three changes in 24 h).

RESULTS

Formation of Monolayers

Monolayers of MDCK cells were obtained by plating cells harvested from roller bottles containing confluent cultures onto collagen-coated disks. The very high cell density used for plating (10^6 cells/cm^2) was more than sufficient to saturate the area of substrate available for attachment, but, as expected from the fact that upper cell surfaces of epithelial lines do not support the attachment of other cells (28), only a monolayer was formed. When disks were transferred to fresh medium after 90 min at 36.5°C, no large uncovered areas of collagen were visible by light microscopy on the surface of the disks, although scanning electron microscopy revealed small spaces between cells and occasional clumps of cells.

After 48 h, monolayers that formed on the plastic surface outside the disks developed transient domes or blisters similar to those described by Leighton et al. (50, 51) in monolayers formed by growing the cells to confluence directly on a glass or plastic surface. The blisters were sometimes visible to the naked eye and were easily apparent by phase (Fig. 2*a*) or scanning electron microscopy (Fig. 2*b*). Leighton and his collaborators (50, 51, 1) have suggested that blisters result from the vectorial movement of water from the medium toward the glass side on which water accumulates. Support for this notion is obtained from the fact that domes or blisters were absent at all times from monolayers formed on the permeable support provided by the collagen-coated disks (Fig. 3).

Light micrographs of cross sections of disks (Fig. 3*a* and *b*) showed that 48 h after plating, the cell layer was only one cell thick (i.e., a true monolayer), and that there were no cells attached to the undersurface (Fig. 3*a*). Scanning electron

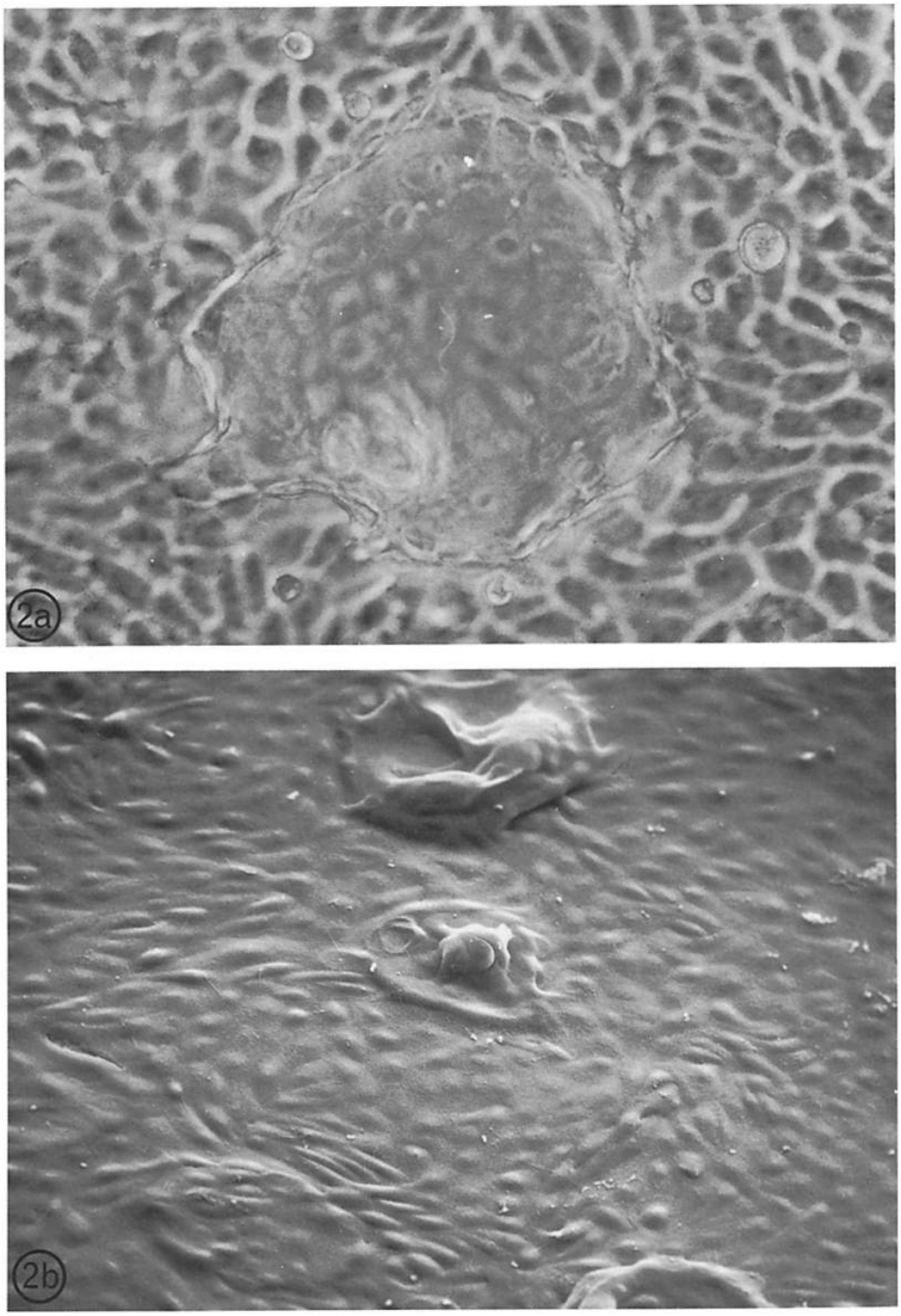

FIGURE 2 (*a*) A phase photomicrograph showing one dome or blister (above the plane of focus) in an MDCK monolayer. The appearance of blisters is typical of MDCK monolayers grown on impermeable supports. × 700. (*b*) Scanning electron micrograph of an MDCK monolayer grown on a plastic Petri dish. Several blisters, some partially collapsed during processing, are visible. × 242.

micrographs showed no discontinuities in the cell layer (Fig. 3 *c* and *d*). Most cell surfaces appeared generally flattened and with polygonal contours, although some rounded cells were present (Fig. 3 *c* and *d*). It was not possible to determine whether the rounded cells were undergoing mitosis or whether they had attached to the substrate but because of the high plating density, had not been able to spread.

Thin-Section Electron Microscopy

A morphological polarization of MDCK cells was apparent in transmission electron micrographs of cross sections of monolayers (Fig. 4 *a*). Nuclei were located toward the collagen side, whereas most cytoplasmic organelles were abundant in the upper halves of the cells and Golgi apparatus were located preferentially toward the lateral aspects. This observation is in contrast to that of Misfeldt et al. (59) that in MDCK monolayers grown on Millipore filters, nuclei and cellular organelles are not asymmetrically distributed. On the free surface of the monolayers, characteristic microvilli containing microfilamentous cores were present, and in a few cases, cilia were found. The basal aspects of the cells did not project into the collagen layer (Fig. 4 *a*) whereas in monolayers grown on Millipore filters, cell processes partially penetrate into the pores of the filters (59). A thin layer of amorphous material was observed between cells and the collagen substrate (Fig. 4 *a*). This probably corresponds to the "microexudate" reported for MDCK cells (63). Basolateral aspects of the plasma membrane showed frequent processes, interdigitations with neighboring cells, and desmosomes (Fig. 4 *a, b,* and *c*). Intercellular spaces were of variable width (200–600 nm) and appeared closed at the free surface of the monolayer by junctional complexes composed of occasional desmosomes and tight junctions (zonulae occludens) (Fig. 4 *a* and *b*).

The permeability of the junctional complexes to macromolecular tracers was tested with lactoperoxidase (Fig. 5 *a*) and colloidal lanthanum (Fig. 5 *b* and *c*). When lactoperoxidase was applied to the free side, the reaction product covered the apical surface but did not penetrate into the intercellular space which was totally free of precipitate. This observation suggests that the enzyme probe was unable to completely traverse the tight junctions. When colloidal lanthanum was applied from either side of the monolayer, small amounts of the tracer were regularly found within zonulae occludens (Fig. 5 *b* and *c*). The images suggested that lanthanum diffused through the tight junctional strands and remained trapped within the zonulae occludens while it was removed from other portions of the intercellular spaces during subsequent processing. Other studies have shown that colloidal lanthanum crosses tight junctions of leaky epithelia such as rabbit gallbladder and intestine (53), and rat proximal and distal convoluted tubules (57).

Freeze-Fracture Electron Microscopy

As mentioned above, zonulae occludens sealed the intercellular spaces from the luminal compartment to which the microvilli were exposed. Freeze-fracture replicas of monolayers showed, as reported by Misfeldt et al. (59), typical tight junctions in both E and P fracture-faces (12) near the luminal side of the intercellular spaces (Fig. 6 *a–c*). In specimens in which the fracture plane crossed the intercellular space, it was apparent that ridges of intramembranous particles in P fracture-faces formed networks which were in register with corresponding grooves in the E faces (Fig. 7 *a*). The complexity of the branching pattern and the number of intramembranous strands varied extensively within very short distances (a few nanometers) along the zonula occludens (Figs. 6 *a–c* and 7 *c*). Sometimes only one or occasionally two or three parallel strands were observed, whereas in other instances, up to seven rows of interconnecting strands were present in one fracture-face. Strands frequently showed loose ends (Figs. 6 *a* and 7 *c*) and at times formed open and closed loops. Although most strands appeared as continuous ridges of particles in the P face, regions in which the strands had a fragmented or even a beaded appearance were common (Fig. 7 *a*). Similar variations have been observed in natural kidney epithelia (64). In some cases in which both fracture-faces were seen in the same replica, it was apparent that when junctional strands appeared fragmented in the P face, more particles were seen in the junctional grooves of the E face (Fig. 7 *a*).

At the free surface of the monolayer, fingerlike processes or microvilli of adjacent cells frequently interdigitated while lying over the surface of the neighboring cell. Tight junctions formed along the regions of contact outlining these processes (Fig. 7 *b*). The junctional strands of these outlined processes appeared to run in the free surface plasmalemma at right angles to the main part of the junction (Figs. 6 *c* and 7 *b*).

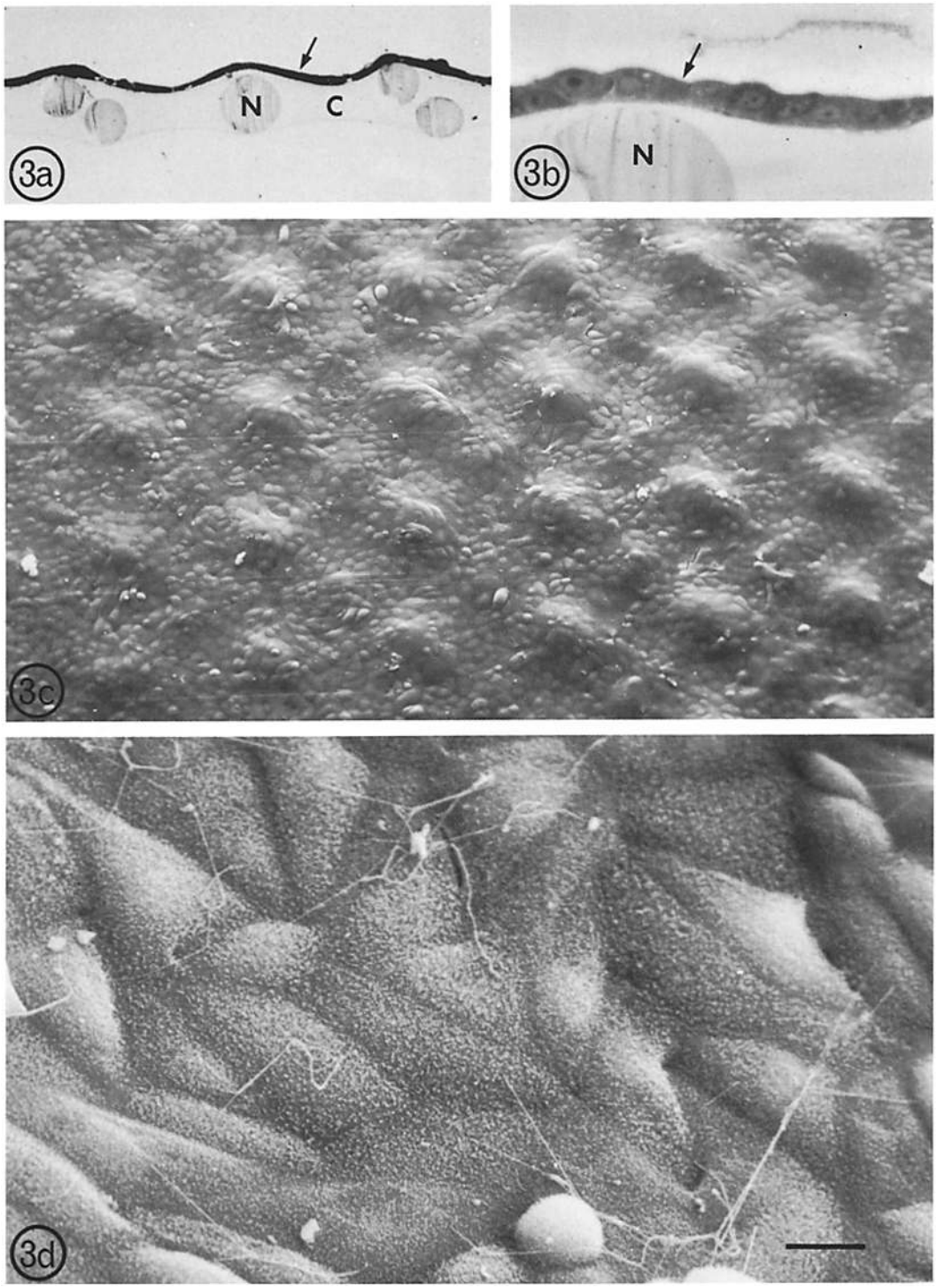
N
C
3a
N
3b
3c
3d

As mentioned above, desmosomes were often seen near the tight junctions, as well as along other portions of the membranes facing the intercellular spaces. The appearance of desmosomes in freeze-fracture replicas consisted of macular areas of aggregated intramembranous particles of various sizes (Fig. 7*a*) similar to those of stratified squamous epithelia (73, 46).

Electrical Measurements

Electrical measurements (Fig. 8) indicated that a resistance began to develop in the monolayer during the first 4–6 h after plating. The value of this resistance rose continually during the first 24 h, at the end of which period it reached a maximum (~340 $\Omega \cdot cm^2$). The resistance then decreased to a value of 104 ± 1.8 $\Omega \cdot cm^2$ (number of observations (n) = 219) which was reached after 30 h. This value remained constant for up to a month after plating. The value of the resistance was unaffected by the conditions of measurement for up to 2 h in the chamber (Fig. 9). This paper is primarily concerned with the structure and properties of the monolayer in steady state (after the first 30 h). The results reported here were obtained with monolayers 2–10 days after plating. Events during the early stages (i.e., the first 30 h) will be described separately.[1]

Values of the conductance per unit area calculated for chambers with different-sized openings (0.1–0.9 cm^2) were independent of the exposed area in chambers. This indicates that the effect of "edge damage" (29) is negligible. Indeed, scanning electron micrographs of the edge of the disk showed minor abrasions limited to the raised areas of the surface (not illustrated). The resistance at steady state was not significantly affected by changes in temperature between 21°C (108.8 ± 4.6 $\Omega \cdot cm^2$ [n = 12]) and 36.5°C (115.4 ± 4.3 $\Omega \cdot cm^2$ [n = 11]). Misfeldt et al. (59) have reported for monolayers of MDCK cells grown on Millipore filters a mean transepithelial electrical resistance of 83.7 ± 1.2 $\Omega \cdot cm^2$ at room temperature and 61 ± 10 $\Omega \cdot cm^2$ when measurements were made at 37°C.

Spontaneous electrical potentials ($\Delta\Psi$) generated by MDCK monolayers prepared by heavy plating varied considerably but were seldom larger than 1.0 mV (collagen or "inner" side positive) (Table I). This low value is in agreement with the mean value of 1.42 ± 0.260 mV reported by Misfeldt et al. (59) and with the expectation for a leaky epithelium in which the high conductance of the paracellular pathway acts as a shunt (2, 62, 71).

The value of $\Delta\Psi$ was decreased by the addition of amiloride, a specific inhibitor of Na^+ movement across epithelia (Fig. 10). The concentration employed (5×10^{-5} M) was selected from the affinity study of Salako and Smith (69). In natural epithelia, the effects of this dose are usually reversible (26). Amiloride is known to act on the free ("outer") side of epithelia (30, 18). In these experiments, however, it was added to both sides of the MDCK monolayer to avoid creating an asymmetry which might influence the small $\Delta\Psi$. As illustrated in Fig. 10, in contrast with most natural epithelia (7), the effect of amiloride was not fully reversible. However, the fraction of the voltage inhibited by successive additions and washings of amiloride was constant. In a set of 10 monolayers, amiloride produced a decrease of 65.1 ± 5.5% (n = 10) of the total $\Delta\Psi$, suggesting that about two-thirds of the value of $\Delta\Psi$ is due to Na^+ movement.

To test the ability of the monolayers to discrim-

[1] Manuscript in preparation.

FIGURE 3 (*a* and *b*) Light micrographs of transverse sections (0.5 μm) of an Epon-embedded confluent monolayer on a collagen-coated disk. Note that the nylon fibers (*N*) are embedded in the collagen layer (*C*), that the cell layer is complete, and that there are no cells on the lower surface of the disk. Arrow points to the monolayer. (*a*) × 175; (*b*) × 490. (*c*) Scanning electron micrograph of a monolayer of MDCK cells, formed by plating on a collagen-coated nylon disk. Domes are absent. The prominences correspond to the raised fibers in the nylon cloth which are also coated with collagen and covered with cells (cf. Fig. 1). Rounded cells are frequently seen. These may be cells in mitosis or cells which are attached but were unable to spread. × 97.5. (*d*) Scanning electron micrograph of the upper surface of a complete monolayer such as that seen in Fig. 3*c*. Cells appear to bulge gently in their nuclear region and are covered by a mat of short, irregular microvilli. Precise lateral borders are difficult to discern. This may be due to the fact that, to a great extent, near their luminal surface cells overlap and interdigitate as seen in the transmission electron micrographs of transverse sections (Fig. 4*a*). A rounded cell in the lower right may be in mitosis. × 1,260. Bar, 10.0 μm.

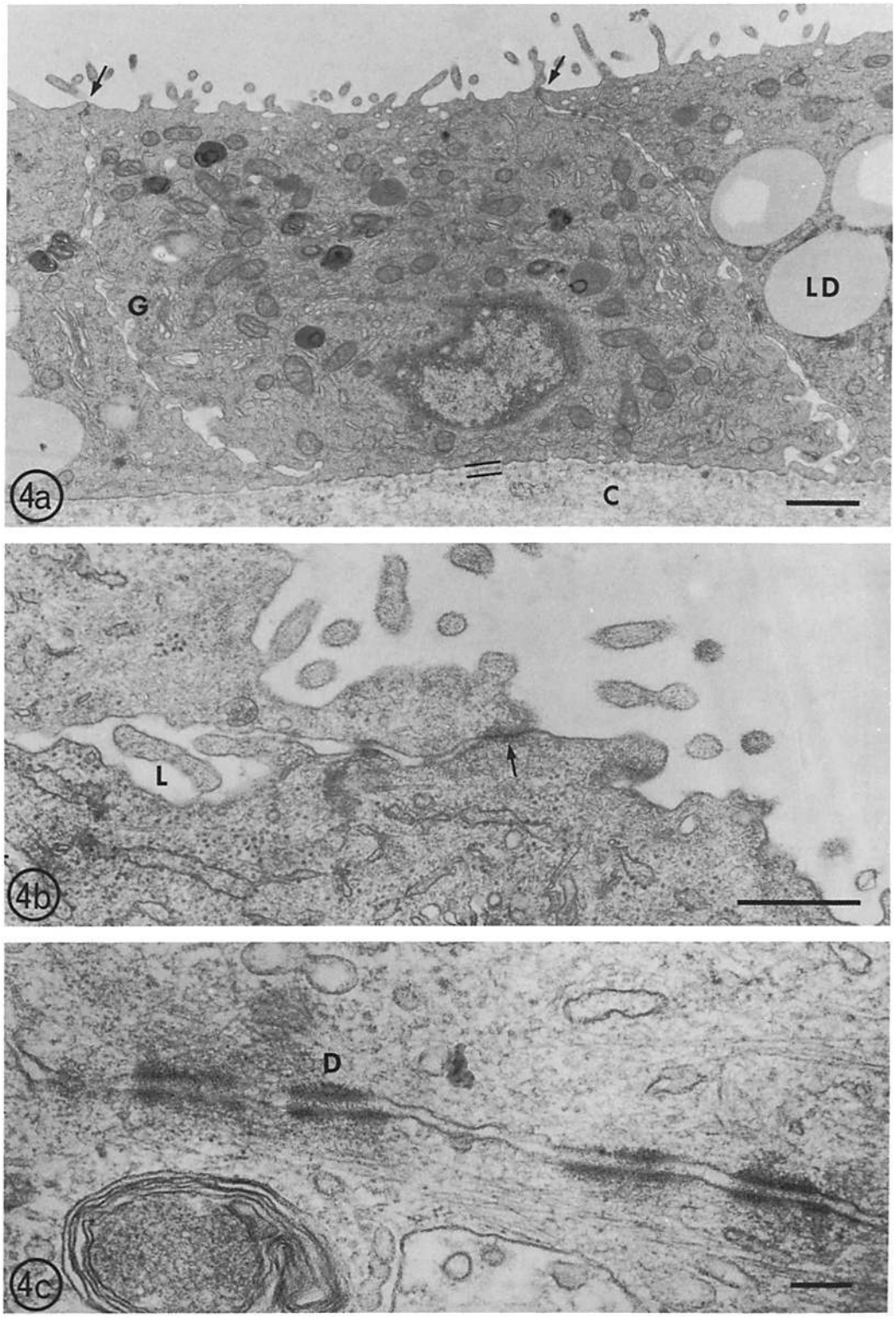
G
LD
C
4a
L
4b
D
4c

inate between anions and cations, the ratio (β) between the permeability to chloride (P_{Cl}) and that to sodium (P_{Na}) was calculated. The dilution potential generated by mounting the preparation between two different isotonic Ringer's solutions containing 150 and 75 mM NaCl was measured. The relationship between the dilution potential ($\Delta\Psi$) and β is given by the Hodgkin-Huxley version of Goldman's constant field equation:

$$\Delta\Psi = \frac{RT}{F} \ln \frac{a^o_{Na} + \beta a^i_{Cl}}{a^i_{Na} + \beta a^o_{Cl}} \qquad \beta = \frac{P_{Cl}}{P_{Na}} \qquad (2)$$

where a^o and a^i are the chemical activities in the outer and the inner solutions, respectively. With the measured value of $\Delta\Psi$ (12.00 ± 0.61 mV [n = 15]), β was equal to 0.11, indicating that the preparation is eight to nine times more permeable to Na^+ than to Cl^-. The absolute value of the dilution potential of the monolayer of MDCK cells was independent of the orientation of the salt gradient. Measurements of Na^+ and Cl^- permeability in collagen discs without cell layers gave no evidence of discrimination between Na^+ and Cl^-.

The lower permeability of the monolayer to Cl^- than to Na^+ was also manifested when the streaming potential of five membranes with an average resistance of 132.6 ± 24.8 $\Omega \cdot cm^2$ (n = 5) was studied. Streaming potentials are thought to be largely boundary diffusion potentials due to flow-induced solute concentration changes in unstirred layers of the epithelium (82). The streaming potential measured was −0.83 ± 0.13 mV (collagen side negative, n = 5) when 50 mosmol of glucose was added to the MEM bathing the free ("outer") side. This observation suggests that the restriction exerted by the junctions on the ions is greater on anions than on cations, and therefore, the outer side becomes positive with respect to the inner (collagen) side. Misfeldt et al. (59) measured streaming potentials after creating with sucrose 50- and 100-mosM gradients and obtained values which are lower than those reported here. The possibility cannot be totally discarded that, in our experiments, glucose stimulates a Na^+-transport mechanism through the cells from the basal to the outer compartment which would make a contribution to a potential of direction similar to that observed.

Water Flux

A net water flux from the free to the collagen side was detected in the absence of osmotic and hydrostatic gradients and at 22°C, across monolayers mounted in between two identical media (CMEM). In three preparations, the value of the net inward flux was: 12.7, 25.9, and 20.7 μl/h per cm^2. In monolayers grown on Millipore filters, Misfeldt et al. (59) measured at 37°C a net water flux of 7.2 ± 3.5 μl/h per cm^2 (n = 15) in the apical to basolateral direction.

Role of Ca^{++}

Fig. 11 illustrates the effect on the resistance of replacing CMEM with Ca^{++}-free MEM containing EGTA (2.5 mM) on both sides of the monolayer. An initial sharp drop of resistance was followed by a slower decay which was reversed when Ca^{++} was restored. To assess independently the relative effects of Ca^{++} removal and chelation with EGTA, separate disks were incubated in Ca^{++}-free medium, in Ca^{++}-free medium containing EGTA, or in CMEM as controls (Table II). Removal of Ca^{++} led to a drop in resistance of ~27% of the control value within a 2-h period. However, incubation with EGTA almost completely abolished the resistance, suggesting that Ca^{++} ions are involved in maintaining the resistance of the junctions and are not in free equilibrium with Ca^{++} ions in the bathing solution. Replacement with normal Ca^{++}-containing me-

FIGURE 4 (*a*) Portions of three cells from a confluent monolayer formed by plating on a disk. The apical surfaces bear short, irregular microvilli. The lateral spaces are sealed off from the upper compartment by junctional complexes composed of tight junctions (arrows) and desmosomes. Note the presence of Golgi apparatus near the lateral surfaces (*G*) and the presence of lipid droplets (*LD*). Basally, the cells rest on a thin, darkly staining "microexudate" (in between thin parallel lines) layer probably of their own manufacture, separating them from the collagen (*C*). × 11,250. Bar, 1.0 μm. (*b*) Detail of the tight junction region (arrow) of two MDCK cells. Basal to the tight junction, the lateral space is somewhat open (*L*) and shows fingerlike processes. × 38,000. Bar, 0.5 μm. (*c*) Desmosomes (*D*) are present under the tight junction but also form adherent spots along the lateral border between MDCK cells. Note filaments in the adjacent cytoplasm. × 90,000. Bar, 0.1 μm.

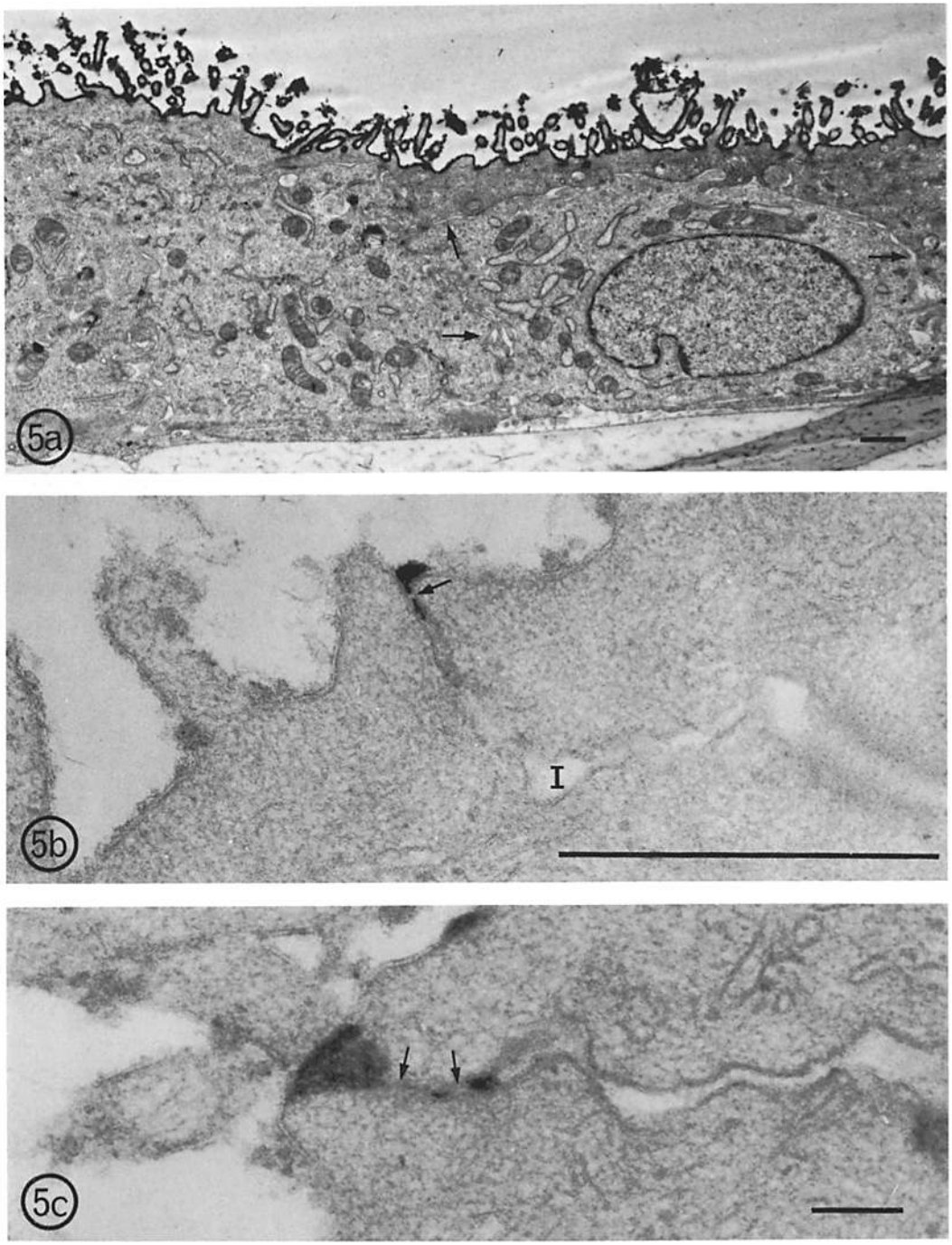

FIGURE 5 (*a*) Low magnification micrograph of a section of an MDCK monolayer which had lactoperoxidase applied to its upper surface. The dense precipitate corresponding to the reaction product using DAB outlines the free surface of the monolayer and microvilli but does not enter the lateral spaces (arrows). × 6,600. Bar, 1.0 μm. (*b*) Transmission electron micrograph of an MDCK monolayer on a collagen-coated nylon disk which had colloidal lanthanum applied to the upper surface. Most of the lanthanum was washed away during subsequent processing but small amounts remained in the region of the tight junction. Note that lanthanum penetrated deeply into the junction toward the intercellular space (*I*) and traversed or circumvented at least one tight junction strand (arrow). × 112,200. Bar, 0.5 μm. (*c*) Lanthanum deposits within a tight junction region from the same monolayer as described in Fig. 5*b*. Note that here the marker is found beyond at least two tight junction strands (arrows). × 135,000. Bar, 0.1 μm.

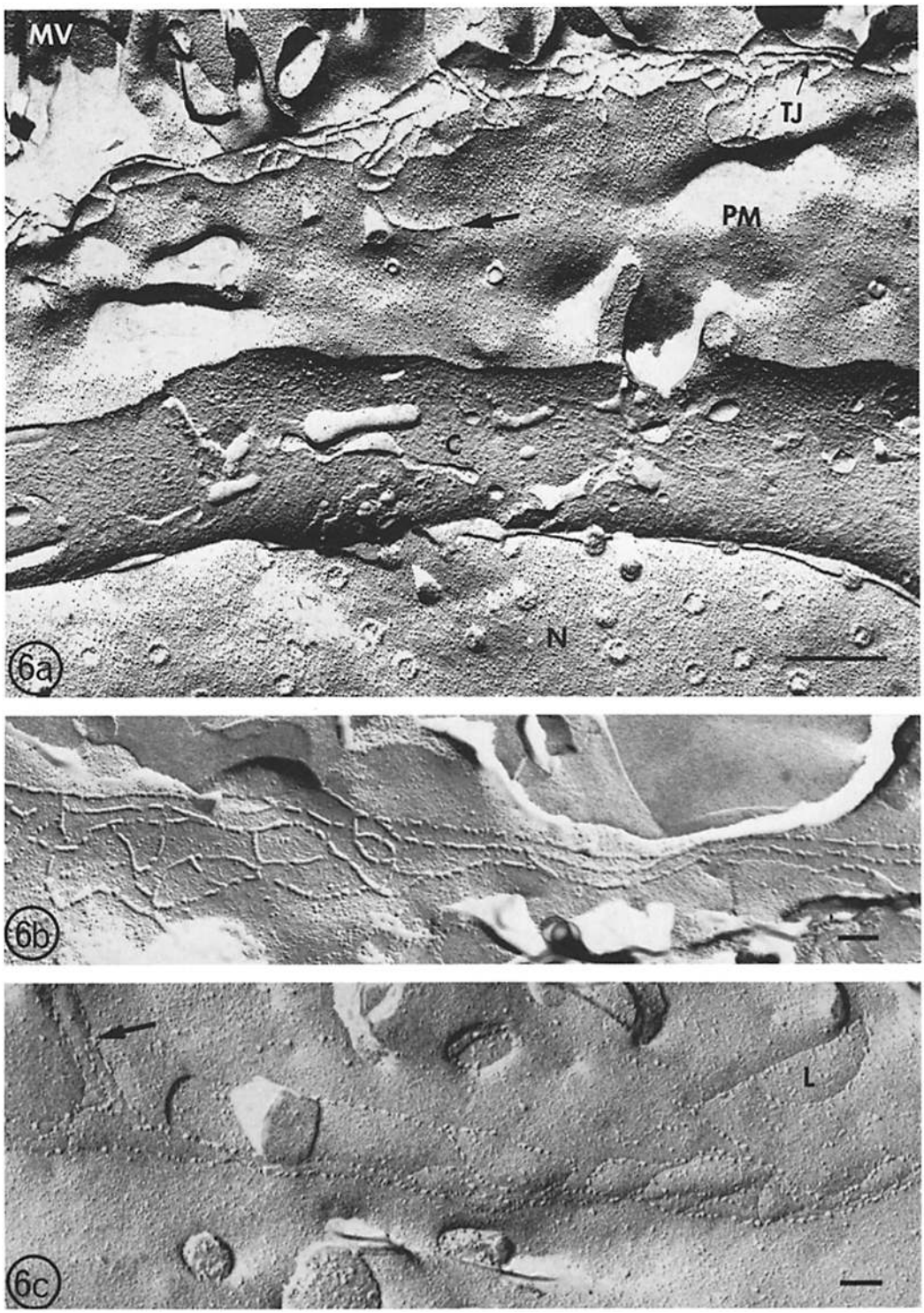

FIGURE 6 (*a*) Freeze-fracture replica of an MDCK cell in a confluent monolayer. In the P face of the plasmalemma (*PM*), the tight junction (*TJ*) is seen just below the region of microvilli (*MV*). The fracture plane has also cleaved a region of lateral plasma membrane (*PM*) just below the tight junction region. *C*, cross fractured cytoplasm; *N*, inner nuclear membrane. The junctional strands vary in number and have regions of irregular looping. Note the loose segment of one strand (arrow). × 30,000. Bar, 0.5 μm. (*b*) Tight-junctional strands in a P fracture-face, of an MDCK cell from a confluent monolayer. To the right of the micrograph, three strands are evenly spaced and run parallel to each other. On the left side, strands of this junction show fragmentation and irregular interconnections. × 60,000. Bar, 0.1 μm. (*c*) View of an MDCK tight junction in an E fracture-face. Note that the grooves contain many intramembranous particles. A side branch (arrow) is marked on the left and a closed loop (*L*) on the right. × 60,000. Bar, 0.1 μm.

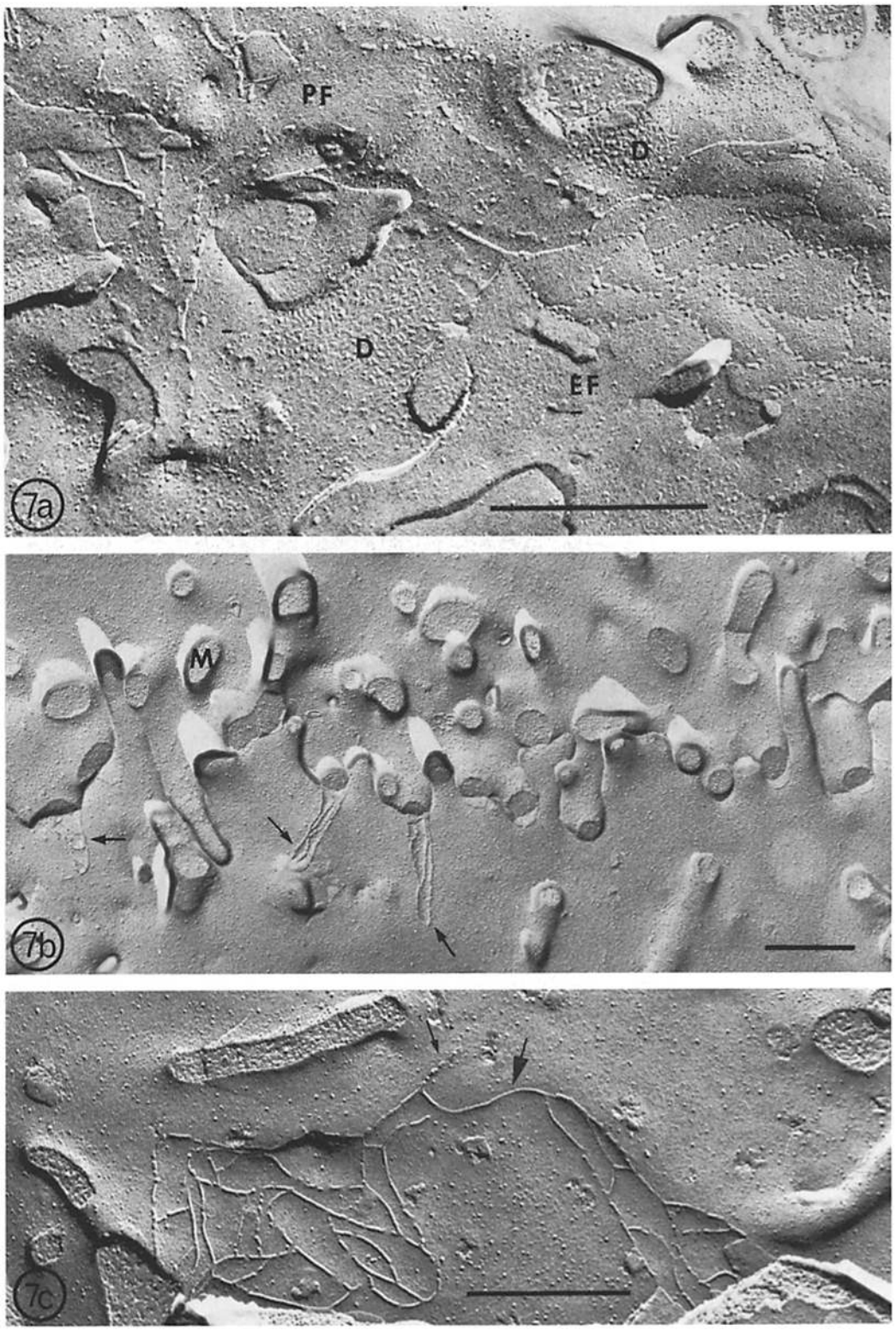
PF
D
D
EF
7a
M
7b
7c

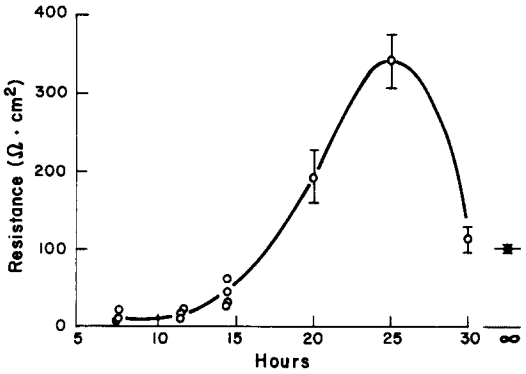

FIGURE 8 Development of electrical resistance in monolayers of MDCK cells plated at high density on collagen-coated nylon disks. At different times of incubation at 36.5°C, disks were mounted between two Lucite chambers containing CMEM for electrical measurements. The area of monolayer exposed to the chamber was 0.2 cm^2. Resistance was calculated from the current necessary to produce a voltage change of 10 mV. All values reported correspond to those of the cell layer and were obtained by subtracting the contribution of a blank collagen-coated disk. Measurements were performed at room temperature (21°C). On the right, the filled circle on the short horizontal line represents the mean value of the resistance in 219 mature monolayers (plated at least 2 days in advance). Zero time corresponds to the time of plating.

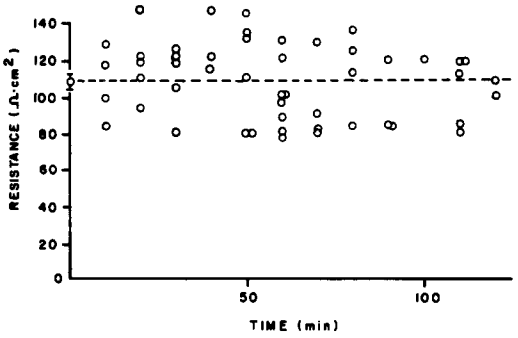

FIGURE 9 Electrical resistance of monolayers of MDCK cells at various times after mounting in the chamber. This figure includes values obtained from monolayers which were used in different experimental tests and remained mounted for different periods of time. The relative constancy of the values illustrates the stability of the monolayers. Measurements were performed as described in Fig. 8. The value at zero time of $109.5 \pm 3.0\,\Omega \cdot cm^2$ ($n = 49$) represents the average for all the monolayers included in the figure of the resistances measured immediately after mounting in the chamber.

dium and incubation at 36.5°C for 15 h led to a restoration of normal levels of resistance in disks preincubated in Ca^{++}-free medium, while the resistance of the group pretreated with EGTA rose to levels significantly higher ($P < 0.05$) than in controls. Electron microscope observations of EGTA-treated monolayers showed areas where junctional complexes between cells were open and intercellular spaces were widened (Fig. 12*a* and *b*).

Effect of Hyperosmolarity

The effect of a hypertonic solution on the electrical resistance of an epithelium may be used to assess the contribution to the resistance of intercellular spaces. Thus, in the gallbladder, where the resistance of the intercellular space is much lower than that of the tight junctions, an expansion of the space produced by hypertonic solutions applied to the serosal side causes no change in electrical resistance. On the other hand, a reduction of the space produced by hypertonicity on the mucosal side elicits a marked increase of the total resistance (75). In very leaky epithelia where the intercellular space contributes signifi-

FIGURE 7(*a*) Replica of a fractured MDCK monolayer showing portions of a tight junction in the P (*PF*) and E faces (*EF*) of membranes of adjacent cells. Note that junctional strands in the PF and grooves in the EF appear for the most part very fragmented and that particles are present in both. D = desmosomes. × 66,000. Bar, 0.5 μm. (*b*) Freeze-fracture micrograph of the luminal plasmalemmas (P faces) of two adjacent MDCK cells. The line of contact between the two cells above the tight junction region runs horizontally across the center of the micrograph. Many fingerlike processes of adjacent cells interdigitate and lie apposed to the luminal plasmalemmas of the cells. Tight-junctional strands exist in areas of contact and are seen in the fractures outlining the shape of the processes (arrow). M = cross-fractured microvilli. × 28,000. Bar, 0.5 μm. (*c*) P-face view of a complex MDCK tight junction with continuous and occasionally interrupted strands. At the large arrow, the junction appears to consist of only one strand. The small arrow indicates the fragmented end of a strand which may represent degradation, formation, or extension of the strand. × 50,000. Bar, 0.5 μm.

cantly to the total resistance, experimental dilation produces a considerable decrease in the resistance. The application of hypertonic solutions to the inner, outer, or both sides of MDCK monolayers produced a clear and reversible increase in electrical resistance (Fig. 13). Treated monolayers were fixed *in situ* by the addition of glutaraldehyde to both sides and examined by electron microscopy. It was found that in all cases hypertonic treatment led to a collapse of the intercellular spaces. Therefore, the effect of hyperosmolarity on either or

TABLE I

Electrical Resistance and Spontaneous Electrical Potential of Monolayers of MDCK Cells

	Resistance*	Potential‡ $\Delta\Psi$
	$\Omega \cdot cm^2$	*mV*
	109	1.5
	143	0.9
	161	0.9
	228	0.9
	102	0.9
	95	0.9
	123	0.8
	114	0.8
	140	0.6
	123	0.6
	179	0.4
	87	0.2
	133.7§ ± 11.6	0.78 ± 0.09
n	12	12

* Calculated as indicated in the legend to Fig. 8.

‡ Collagen side positive.

§ Results are given as mean ± standard error (number of observations).

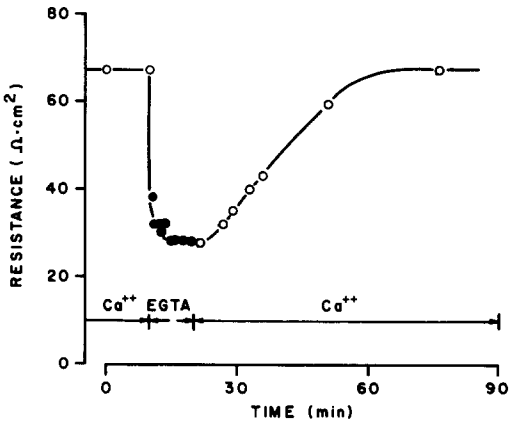

FIGURE 11 Effect of Ca^{++} removal and addition of EGTA on the electrical resistance of a monolayer of MDCK cells. Replacement of CMEM by Ca^{++}-free MEM containing EGTA produced a sharp drop of resistance to half its control value, followed by a slower decrease. Upon return to normal medium containing Ca^{++}, the resistance regained its control value. In between solutions, the chamber was washed three times with the new medium. Changes of the outer and inner solutions were made symmetrically and simultaneously.

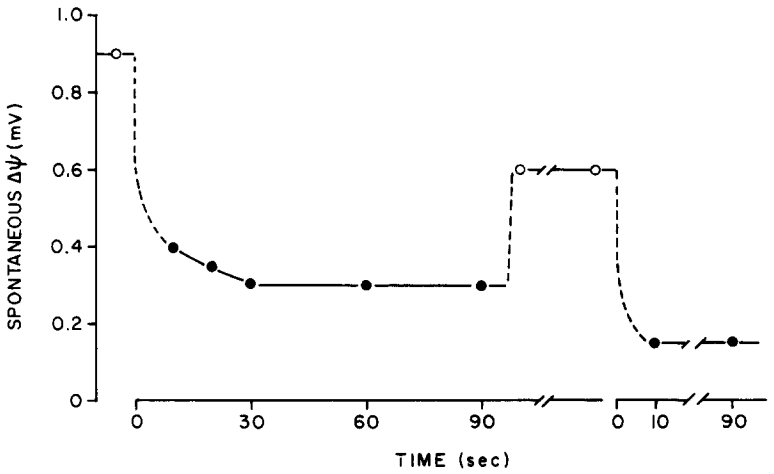

FIGURE 10 Effect of amiloride (5×10^{-5} M) on the spontaneous electrical potential ($\Delta\Psi$) of a monolayer of MDCK cells. In this particular case, the monolayer had an initial $\Delta\Psi$ of 0.90 mV (collagen side positive). Within 30 s after the addition of the drug, the $\Delta\Psi$ decreased to 0.25 mV (●). Removal of amiloride did not fully restore the original $\Delta\Psi$, which remained at 0.60 mV even after several changes of fresh CMEM (○). New addition of amiloride reduced $\Delta\Psi$ to 0.15 mV.

TABLE II

*Effect of Ca^{++} and EGTA on the Electrical Resistance of Monolayers of MDCK Cells**

Length of incubation	Control CMEM	Ca^{++}-free MEM	Ca^{++}-free MEM + EGTA
h		$\Omega \cdot cm^2$ *n*	
2	74.7 ± 0.9 (7)	54.8 ± 1.0 (4)	2.9 ± 0.2 (6)
17	74.6 ± 1.7 (4)	69.9 ± 2.0 (6)	87.8 ± 4.8 (6)

See also legend to Fig. 11.

* Electrical resistance was measured after monolayers were incubated for 2 h in the media indicated, and after the media were replaced by CMEM containing normal Ca^{++} levels and incubation was continued for an additional 15 h.

both sides of MDCK monolayers was similar to that of hyperosmolarity on the mucosal side of the gallbladder. The observations illustrate the free accessibility of the epithelial cells from both sides, but do not clarify the contribution of the intercellular space.

Effect of NaCl Concentration on the Electrical Conductance

The effect of salt concentration on the conductance was studied in a series of MDCK monolayers mounted between identical solutions of NaCl, using mannitol to keep the osmolarity constant.

As shown in Fig. 14, the conductance increased linearly with the activity of NaCl. In this respect, monolayers resemble natural leaky epithelia such as rabbit intestine (70), gallbladder (87), or bullfrog choroid plexus (86). This result suggests that, if the thickness of the permeability barrier is considered equal to that of the beltlike region occupied by all the strands within the zonulae occludens (200–600 nm), the barrier does not contain charged sites, as these would result in a nonlinear conductance/concentration relationship (78, 3).

Instantaneous Current/Voltage Relationship

The instantaneous current/voltage (I/V) relationship was determined for MDCK monolayers (Fig. 15) by delivering increasingly higher current pulses of 20–25 ms in both directions. At the end of the series, a small pulse of current was delivered again to rule out the possibility that the high currents had damaged the preparation. Most voltage curves produced by the square pulses of current reached a plateau in <2 ms. Occasionally, as current pulses became more intense, the voltage curve reached a maximum and then gradually decreased to a steady value. This phenomenon has also been observed in natural epithelia (82, 5, 87) where it was attributed to the transport number effect (changes in the distribution of ions within the unstirred layers, produced by the applied current).

Instantaneous current/voltage curves obtained with MDCK monolayers bathed in symmetrical salt solutions were linear and symmetrical (Fig. 15*a*) within the range of voltage tested (up to 559 mV, five cases) and did not reach saturation, indicating that charged carriers are not involved in ion permeation (24, 25, 33), which suggests the existence of channels.

The I/V relationship was asymmetrical and a small departure from linearity was noticed when monolayers were mounted between solutions of different NaCl concentration (150 vs. 30 mM, keeping the osmolarity constant with mannitol). When the applied current made positive the side with the lower concentration of NaCl, the resistance of the monolayer was greater than when current was passed in the opposite direction. A typical example of such behavior by a monolayer is shown in Fig. 15*b*. In each of the 11 monolayers studied, the resistance was higher in the same direction. The average of the ratio of slopes from individual experiments was 0.81 ± 0.03 (n = 11). Average values of resistances for each direction were 164 ± 36 (n = 11) and 133 ± 21 $\Omega \cdot cm^2$ (n = 11), respectively. These findings support the conclusion, based on the value of the dilution potentials, that $P_{Na} > P_{Cl}$. The resistance is, therefore, lower when the direction of the current moves Na^+ from the higher to the lower concentration and Cl^- in the opposite direction.

The preceding observations may also be taken to suggest that junctions in the MDCK monolayer do not constitute thick barriers with neutral sites, for Barry and Diamond (3) have demonstrated that such barriers should have a linear current/voltage relationship in either symmetrical or asymmetrical single salt solutions. In this respect, MDCK monolayers differ from other "leaky"

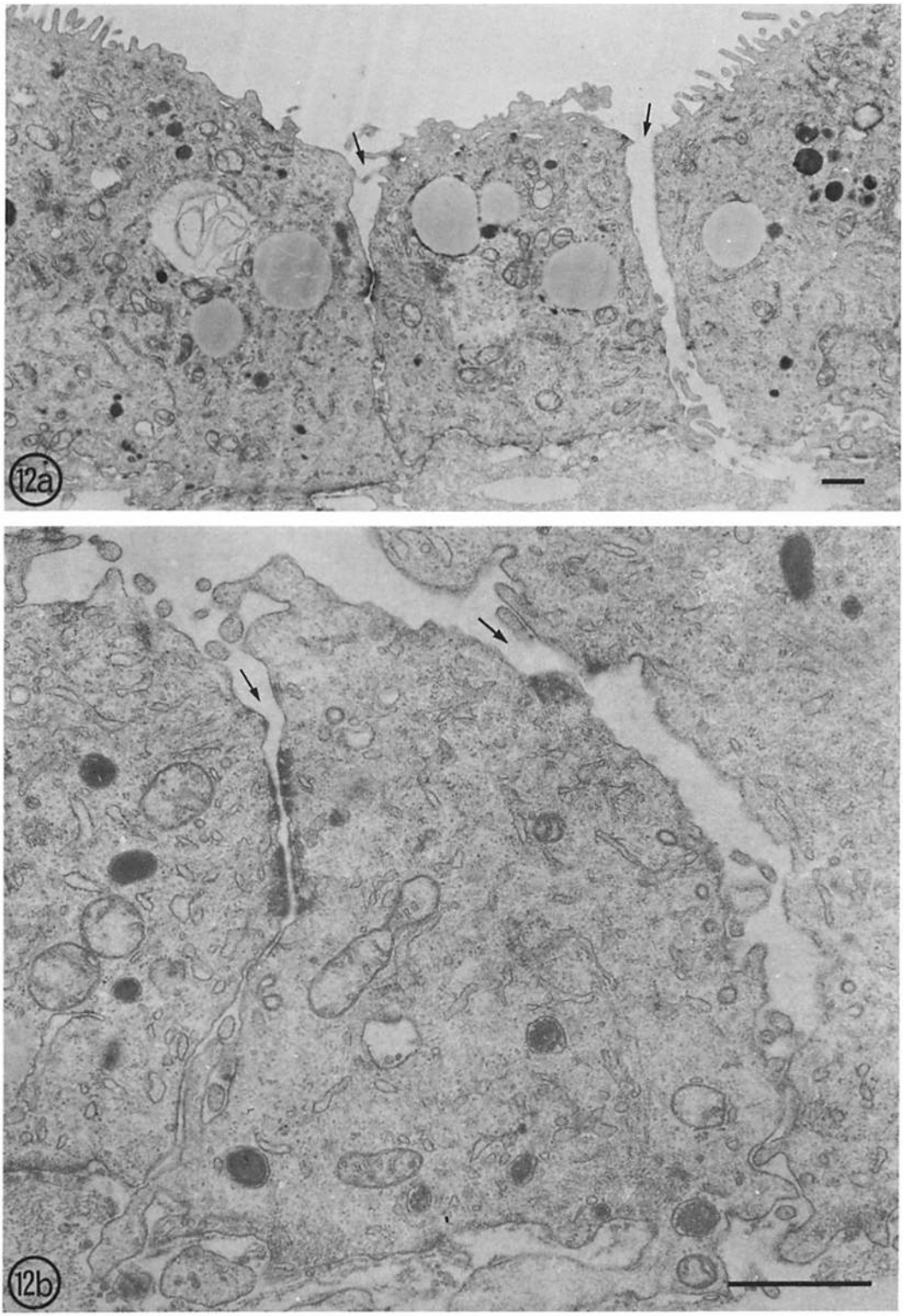

FIGURE 12 (*a* and *b*) Transmission electron micrographs of cells in an MDCK monolayer, treated for 10 min with EGTA in a Ca^{++}-free medium. Tight junctions (arrows) and desmosomes are widely open. Adjacent plasma membranes are separated, and few processes are seen in the intercellular spaces. (*a*) × 6,120; (*b*) × 22,000. Bars, 1.0 μm.

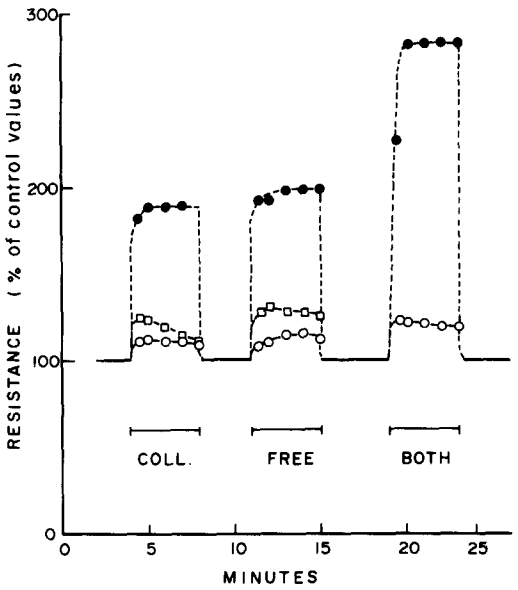

FIGURE 13 Effect of hyperosmolarity on the electrical resistance of monolayers of MDCK cells. Monolayers were mounted between two Lucite chambers containing media stirred vigorously with magnetic bars. Hyperosmolarity was produced by adding sucrose to regular MEM: (●) 300 mM, (□) 150 mM, and (○) 75 mM sucrose. The effect of a solution of given hyperosmolarity was tested after addition to the basal (coll.), apical (free), or both sides of the same monolayer (both). Each change of solution involves three washes with the new solution within 30–40 s. To compare the results obtained under all conditions, values of the resistance measured in the presence of hypertonic solutions are expressed as percent of the values under control conditions (isotonic, regular CMEM) measured before and after each hypertonic treatment. Effects similar to those on the three monolayers illustrated in this figure were observed in 11 monolayers.

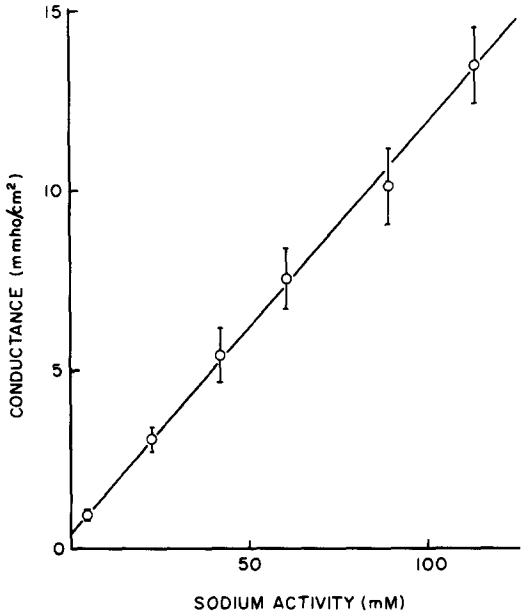

FIGURE 14 Electrical conductance of monolayers of MDCK cells as a function of the chemical activity of NaCl in the bathing solutions. The concentration of NaCl was changed symmetrically and simultaneously on both sides of the membrane. The cells were plated 7 days before the conductance measurements. The area of the chamber used was 0.19 cm^2. Measurements were made at room temperature (21°C).

epithelia such as bullfrog choroid plexus (86) and rabbit intestine (72, 36) in which the $I/\Delta\Psi$ relationship is linear. Nonlinear current/voltage relationships have been found in "tight" epithelia (13, 14) and in thin membranes mounted between two asymmetrical solutions (15). Tight epithelia, however, are not comparable to MDCK monolayers because most of the current does not follow a paracellular pathway (81).

Cation Selectivity: Sequence at Neutral pH

The ability of MDCK monolayers to discriminate among different permeating ion species was examined. For different monovalent cations, the electrical conductance of monolayers mounted between two identical Ringer's solutions containing 150 mM chloride salt was measured. As an example, Fig. 16 presents measurements of the total conductance (G_T) obtained when the least (LiCl) and most (KCl) preferred salts were used. The values of G_T in Table III were obtained similarly, but for a given salt each measurement was preceded and followed by measurements in Ringer's solution with NaCl.

Specific cation conductances (G_+) (Table III) were calculated by subtracting from G_T the fraction of the conductance due to chloride. Chloride conductance for two different salts (NaCl and CsCl) (Table IV) was calculated in a group of eight membranes by measuring G_T and β obtained from the 2:1 dilution potential, as described previously. Since chloride conductance (G_{Cl}) was found to be independent of the nature of the cation, differences in G_T (Table III) can be attributed almost exclusively to differences in G_+ between cations. The observation that G_{Cl} is independent of the cation may also be taken as a suggestion that MDCK monolayers do not contain thick barriers (3).

The sequence of cation conductances found in

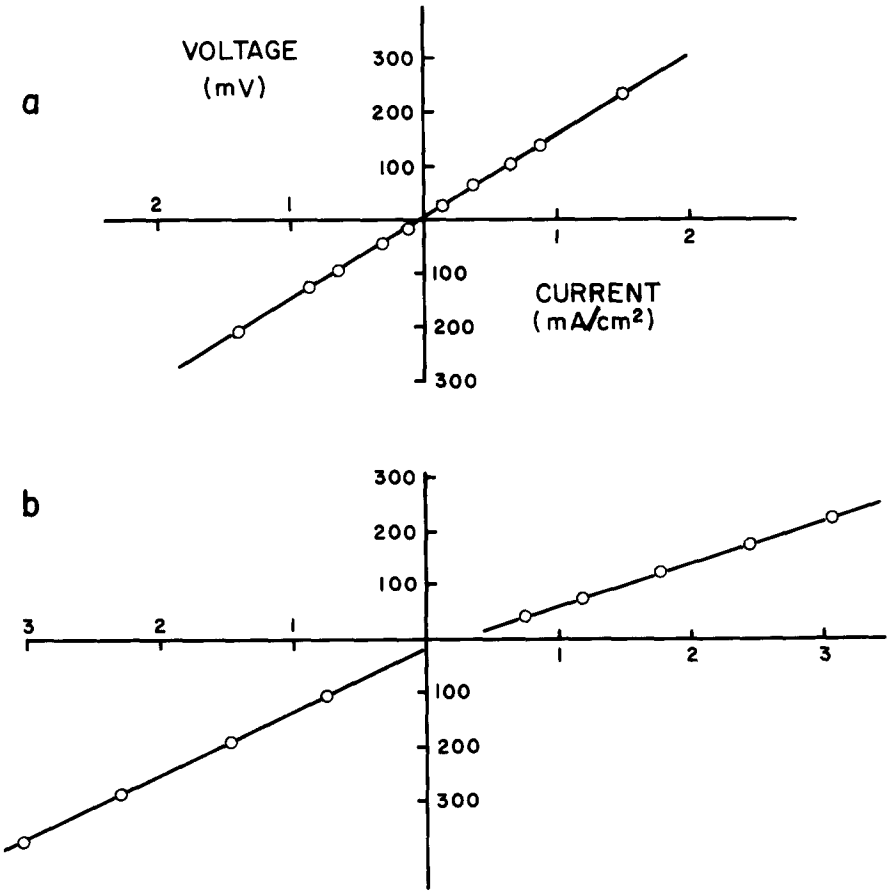

FIGURE 15 (*a*) Current/voltage relationship in a monolayer of MDCK cells mounted between two identical Ringer's solutions containing 150 mM NaCl. The cells in this particular disk had been plated 4 days previously. The slope of the curve is 155 $\Omega \cdot cm^2$. Note the linearity and symmetry of the curve. (*b*) Current/voltage relationship in a monolayer mounted between chambers containing Ringer's solution with 150 mM NaCl on the inner (collagen) side and with 30 mM NaCl on the outer (cell) side. Mannitol was used in the outer solutions to maintain a constant osmolarity. When the inner solution was made positive, the membrane had a resistance of 1330 $\Omega \cdot cm^2$ (upper right). When it was made negative, the resistance was 164 $\Omega \cdot cm^2$. At zero current, the membrane had a negative potential. This is due to its higher permeability to cations than to anions, and the fact that the inner concentration of NaCl was five times higher than the outer.

seven of the eight monolayers studied was $K^+ > Na^+ > Rb^+ > Cs^+ > Li^+$. In the remaining monolayer, the positions of the ions Li^+ and Cs^+ were transposed, resembling the pattern in rabbit gallbladder (4). These sequences differ from that of cation mobilities in free solution ($Cs^+ > Rb^+ > K^+ > Na^+ > Li^+$), indicating that ions do not simply cross through water-filled gaps produced by defective sealing between cells. The sequences found correspond to two (numbers VI and VII) of the 11 (out of 120 possible combinations) predicted by Eisenman (32) on the basis of pure coulombic interactions between anionic sites in the permeability barrier, the mobile monovalent cations, and water molecules. From their position in Eisenman's series, the sequences found suggest that the fields associated with the permeation sites are of intermediate strength.

Eisenman (31, 32) has shown that the degree of hydration of the sites does not alter the order of selectivity in the sequence but reduces the selectivity ratio between the most preferred cation and the least preferred one. In the MDCK preparation, this ratio was only 2.2 (G_K/G_{Li}), suggesting

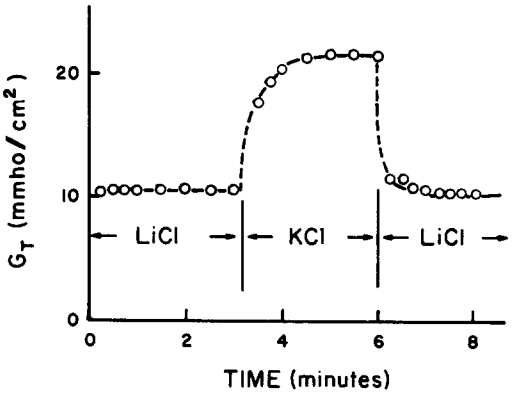

FIGURE 16 Total electrical conductance G_T of an MDCK monolayer placed in Ringer's solutions containing 150 mM LiCl or KCl. Measurements were made 10 days after confluence. The conductance was calculated from the amount of current necessary to produce a voltage change of 30 mV. A measurement in Ringer's solution with 150 mM KCl was made before and after the measurements in Ringer's solution with 150 mM LiCl. Li^+ is the least and K^+ is the most preferred cation.

TABLE III

Cation Selectivity Sequence in Monolayers of MDCK Cells

	G_T	G_+	Relative cation conductance
	mmho/cm² *n*		
K^+	10.84 ± 0.20 (8)	9.34	1.00
Na^+	9.54 ± 0.13 (8)	8.04	0.84
Rb^+	8.48 ± 0.20 (8)	6.98	0.75
Cs^+	6.13 ± 0.21 (8)	4.63	0.50
Li^+	5.66 ± 0.20 (8)	4.16	0.45

The value of the total conductance (G_T) in a solution of the chloride salt of each ion was measured before and after measurements in NaCl solutions. The whole series of salts was tested on each of the eight membranes listed. The value of the cation specific conductance (G_+) was obtained by subtracting G_{Cl} (see Table IV) from G_T.

that the permeation barrier sites are highly hydrated.

The Effect of pH

Changes in the hydrogen ion concentration have been shown to have significant effects on passive ionic conductances in several systems (88, 41, 45). Fig. 17 and Table V show the effect of lowering the pH of the bathing solutions from the control value (7.4) to 3.8. This caused a sharp and reversible decrease of G_T due entirely to a reduc-

TABLE IV

Chloride Conductance G_{Cl} of Monolayers of MDCK Cells

Salt	G_{Cl}
	mmho/cm² *n*
NaCl	1.56 ± 0.16 (8)
CsCl	1.45 ± 0.12 (8)

Total conductance G_T was measured in a solution with 150 mM XCl. A 2:1 dilution potential between isotonic solutions with different concentrations of the same salt was used to calculate the fraction of G_T due to Cl^-. Both measurements were made in each of the eight membranes listed.

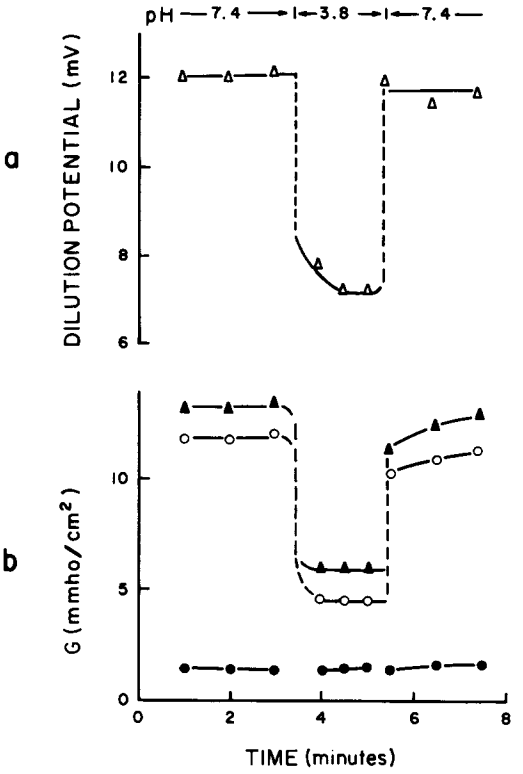

FIGURE 17 Reversible effects of increasing the H^+ concentration to pH 3.8 in a monolayer of MDCK cells 3 days after confluence. Solutions on both sides were of the same pH. (*a*) Dilution potentials calculated with a 2:1 concentration gradient of NaCl (osmolarity maintained with mannitol). (*b*) Total (▲), sodium (○), and chloride (●) conductances (G) calculated with the Goldman-Hodgkin-Katz equation from the amount of current necessary to produce a voltage change of 10 mV and the value of the dilution potential obtained with a 2:1 concentration gradient of NaCl across the membrane.

TABLE V

Effect of pH Changes on Specific Ionic Conductances of MDCK Monolayers

Monolayer	G_{Na}/G_{Cl} at:		
	pH 7.4	pH 3.8	pH 7.4
	mmho/cm²		
1	11.7 ± 1.5	4.7 ± 1.4	10.1 ± 1.3
2	11.7 ± 1.5	4.5 ± 1.6	10.8 ± 1.7
3	12.1 ± 1.4	4.5 ± 1.7	11.4 ± 1.6

G_{Na} and G_{Cl} were calculated on the basis of G_T and a 2:1 dilution potential as illustrated in Fig. 16.

tion of G_{Na}, suggesting that channels involved in Na^+ permeation contain acidic groups which can be protonated. Chloride ions must not cross through these Na^+ channels since their passage is not affected by pH.

Sodium Fluxes

To further characterize the permeation for cations, the unidirectional flux of Na^+, measured in the collagen-to-free surface direction (i.e., outfluxes), was compared with G_{Na} determined electrically. While the first technique measures all Na^+ ions moving across the epithelium, the second reflects the fraction of the flux involving a net transfer of charge. The comparison may be used to put in evidence mechanisms involving mobile sites (carriers) which lead to exchange diffusion, particularly if the mobile sites have a negligible diffusion coefficient in their free state (i.e, when they are not combined with the permeating ion) (33). If the permeating ions form a firmly associated complex with an oppositely charged carrier, the shuttling of this complex would not be reflected in the conductance. In this way, ionic permeabilities measured by trace fluxes would exceed the permeabilities estimated electrically.

Na^+ outfluxes and conductances were measured independently in monolayers mounted between two identical MEM solutions containing 143 or 70 mM NaCl. The measured Na^+ outflux was 6.79 μmol/h per cm² (Table VI). The corresponding P_{Na} calculated as the ratio of the flux to the concentration was 1.72×10^{-5} cm/s. This value should be compared with the P_{Na} that can be calculated from the electrical measurements using the following equation, which describes the relationship between the conductivity of NaCl (G_{NaCl}) and the specific ionic conductivities P_{Na} and P_{Cl}:

$$G_{NaCl} = \frac{F^2}{RT} a_{NaCl}(P_{Na} + P_{Cl}) \quad (3)$$

where a_{NaCl} is the activity of NaCl. This equation is similar to the one derived for thin membranes (Eq. 102 in reference 3). Membranes mounted in Ringer's solution with 143 mM NaCl had a conductivity of 10.0 mmho/cm² (Table VI). ($P_{Na} + P_{Cl}$) is therefore equal to 2.46×10^{-5} cm/s. Combining this value with that for P_{Cl}/P_{Na} obtained with the same batch of membranes ($\beta = 0.11$), the P_{Na} obtained is 2.22×10^{-5} cm/s. For 70 mM NaCl, if one assumes that β does not change with the concentration, P_{Na} values equal to 1.86×10^{-5} and 1.82×10^{-5} cm/s were calculated with the conductivity and flux parameters, respectively. The remarkable agreement between electrical and flux determinations of P_{Na} indicates that exchange diffusion (80) is absent or plays a very minor role in the MDCK preparation.

Comparison with Other Cell Lines

Resistance and permeability measurements were carried out in monolayers formed with epithelial and connective tissue cells of various origins which were plated as described for MDCK cells (Table VII). Only epithelial-like cells appeared able to form monolayers with resistances comparable to those in natural transporting epithelia. An apparent exception was that of SIRC cells, which have a fibroblastic appearance but developed a low value resistance. Among those tested, only monolayers prepared with MDCK cells showed any discrimination between permeating ions as expressed by β. It should be emphasized,

TABLE VI

Sodium Fluxes and Electrical Conductances of MDCK Monolayers Mounted between Two Identical MEM Solutions

Sodium concentration	Na^+ fluxes		Conductance	
mM	*μmol/h/cm²*	*n*	*mmho/cm²*	*n*
143	6.79 ± 0.92	(7)	10.0 ± 1.1	(7)
70	3.77 ± 0.30	(11)	4.5 ± 0.2	(11)

1 μCi of ^{22}Na was added to the solution bathing the collagen side, and radioactivity was measured in aliquots taken at different times from the other chamber. The value of the sodium outflow for a given monolayer was determined from three to five measurements taken at intervals of 10 min. When solutions with 70 mM NaCl were used, osmolarity was maintained with sucrose.

TABLE VII

Characteristics of Monolayers Prepared by Plating Various Cell Types

Cells	Origin	Characteristics	Resistance*		β‡	
			$\Omega \cdot cm^2$	n		n
WI38	Lung, human fetus	Fibroblastlike	0		0	
BHK	Kidney, hamster	Fibroblastlike	0		0	
SIRC	Cornea, rabbit	Fibroblastlike	8.5 ± 0.4	(6)	1.40 ± 0.01	(6)
BS-C-1	Kidney, monkey	Epithelial-like	13.3 ± 1.3	(6)	1.11 ± 0.02	(6)
MDBK	Kidney, bovine	Epithelial-like	83.4 ± 15.8	(9)	1.14 ± 0.01	(6)
MDCK	Kidney, dog	Epithelial-like	104 ± 1.8	(219)	0.11 ± 0.01	(12)

The different cell types were plated at the same density (10^6 cells/cm^2).
Measurements were made 2 days later in CMEM at room temperature.
* Calculated as described in Fig. 8.
‡ Calculated with a 2:1 dilution potential of NaCl and Eq. 2.

however, that no effort was made to develop conditions which may lead to higher resistance with the other cell types. It should also be noted that direct comparisons of resistances cannot be made without taking into account geometric features of the cells and monolayers. For example, other factors being the same, epithelial with smaller cells or with more extensive interdigitations might be expected to have a higher conductivity.

DISCUSSION

The work presented here confirms and extends recent reports (59, 19) showing that uninterrupted monolayers formed by MDCK cells on permeable supports develop and maintain many of the properties found in natural epithelia. Monolayers prepared by the simple procedure described in this paper are ready within 2 days for studying permeability properties in a steady state. Before this time, cellular events leading to the formation of the monolayers can also be followed with relative simplicity, as will be described separately.[1] Mature MDCK monolayers remained functional for several weeks and discontinuities were not detected morphologically or electrically for at least a month. Cell detachment by death or mitosis did not perturb the integrity of the monolayer, probably because repair processes quickly "healed" small gaps, as in "wounds" produced in monolayers and natural epithelia (44, 79, 77).

One of the key features of transporting epithelia is their structural and functional asymmetry. The structural polarity of MDCK monolayers is apparent morphologically, as noted by Misfeldt et al. (59), by the position of microvilli and tight junctions. In addition, in our preparations the orientation of nuclei and subcellular organelles was also asymmetrical. In both types of preparations, the polarity of the monolayers was manifested functionally by a unidirectional water flux and the presence of a small spontaneous electrical potential.

MDCK monolayers withstand most of the current procedures used to characterize the permeability of epithelia. In more than 3 yr of study, we have not observed a single accidental detachment of the cell layer, after disks were mounted in the chambers. Even when addition of EGTA in the absence of Ca^{++} led to an opening of the tight junctions and to a drastic decrease of resistance, cells remained attached to the collagen substrate and were able, upon restoration of normal Ca^{++} levels, to reestablish cell contacts and junctions, as shown by the rise in resistance.

The steady-state value of the resistance of MDCK monolayers (104 ± 1.8 $\Omega \cdot cm^2$) is considerably higher than in many natural epithelia, such as kidney proximal tubules of the dog (5.6 $\Omega \cdot cm^2$) (10), rat (5.7 $\Omega \cdot cm^2$) (43), and *Necturus* (43 $\Omega \cdot cm^2$) (76). However, it is considerably lower than in distal tubules of the rat (150–300 $\Omega \cdot cm^2$) (56) and dog (600 $\Omega \cdot cm^2$) (10) or collecting tubules of the rabbit (867 $\Omega \cdot cm^2$) (43) and hamster (2,000 $\Omega \cdot cm^2$) (65). Because of the value of the resistance, the MDCK preparation may be regarded as a model for "leaky" epithelia, in which passive fluxes proceed almost exclusively through a paracellular pathway, rather than through the cell cytoplasm (37, 71). Smulders et al. (75) and Wiedner and Wright (83) have observed that, in epithelia with low electrical resistances (e.g., 5–20 $\Omega \cdot cm^2$) and narrow intercellular spaces (<100 nm), diffusion along these spaces

may affect the value of the resistance. Because MDCK monolayers have a high resistance (~100 $\Omega \cdot cm^2$) and wide intercellular spaces (200–600 nm), diffusion along these spaces must not contribute significantly to the total resistance. For comparison, in the gallbladder, which has a resistance of only 20–30 $\Omega \cdot cm^2$, <5% of this value is contributed by the paracellular route, most of the resistance being due to the junctions (83).

We found that, when the MDCK preparation was mounted between two compartments containing different NaCl concentrations in isotonic solutions, the absolute value of the dilution potential did not depend on the orientation of the salt gradient. Symmetrical dilution potentials are characteristic of natural leaky epithelia. Tight epithelia such as frog skin (47, 16), toad urinary bladder (49), and frog stomach (42) do not show dilution potentials because the junctional complexes block the paracellular routes. In contrast, in "leaky" epithelia the control of passive permeation through paracellular routes is exerted by tight junctions. Thus, a characterization of the passive permeability of a leaky epithelium becomes a characterization of its junctions.

The permeability barrier formed by the tight junctions was examined in terms of its effective thickness and possible permeation mechanisms. Because estimates of the Na^+ permeability obtained with electrical methods agreed with measurements in which tracers were used, we ruled out an exchange diffusion mechanism of Na^+ permeation involving carriers. The fact that $I/\Delta\Psi$ curves did not reach saturation also indicates (25, 33) that carriers are not involved in Na^+ permeation, and suggests the existence of channels.

Viewed in the light of models now available (4), several properties of MDCK monolayers indicate that their permeability barrier may be regarded as a "thin" membrane containing Na^+ channels lined by negatively charged sites of medium field strength. These properties are: (*a*) the linearity of the conductance/concentration relationship; (*b*) the asymmetry of the $I/\Delta\Psi$ curve in monolayers mounted between asymmetrical but isotonic solutions of the same salt; (*c*) the effect of a decrease in pH which reduces the ability to discriminate between Na^+ and Cl^-; and (*d*) the characteristic pattern of ionic selectivity ($K^+ > Na^+ > Rb^+ > Cs^+ > Li^+ \gg Cl^-$) which corresponds to series VI of Eisenman (32).

The $K^+ > Na^+ \gg Cl^-$ conductance order in the monolayers of MDCK cells is in agreement with that reported by Malnic and Giebisch (56) for the distal tubule of the rat at neutral pH. In the MDCK preparation, the ratio between the conductances of the most and least preferred cations was only 2.2 (G_K/G_{Li}), which is 20–25 times lower than in single plasma membranes (55, 74, 52) and in tight epithelia (17, 18). The low value of this ratio in MDCK monolayers indicates that permeation sites are highly hydrated (31, 33), a feature characteristic of several natural leaky epithelia (4, 61, 62). The ability of the MDCK barrier to discriminate between Na^+ and Cl^- was severely but reversibly decreased by an increase in the H^+ concentration. Thus, at pH 3.8 there was a drastic reduction of P_{Na} without a significant modification of P_{Cl}. These observations suggest that the barrier has Na^+-specific channels which exclude Cl^- and contain acidic groups dissociated at neutral pH. Although the sequence of selectivity found indicates that mobile cations interact with negatively charged sites in the membrane, it cannot be necessarily concluded that the membrane contains *net* negative charges. Negative ends of dipoles facing the permeation channel could also result in an ability to discriminate among cations.

In general, the functional properties of the junctions reveal some striking similarities between the MDCK monolayer and initial portions of the mammalian nephron, although it cannot be concluded on this basis that MDCK cells are derived from a particular portion of the nephron. In preparations of MDCK cells grown on Millipore filters, Misfeldt et al. (59) observed a Na^+ to Cl^- discrimination (t_{Na}/t_{Cl}) of 1.7, similar to that of proximal tubules in dog (1.38) (10) and rat kidney (1.58) (38). In our preparation, however, we measured a much higher discriminating ability between Na^+ and Cl^-. It cannot yet be established whether the two estimates of the selectively obtained reflect differences in the source of cells and methods employed to form the monolayers, including the type of solid support (Millipore filter vs. collagen).

SUMMARY

Our observations and those of Misfeldt et al. (59) show that, morphologically, junctional complexes in MDCK monolayers resemble those in natural epithelia (35, 40, 84, 57). We observed by freeze-fracture that the complex arrangements of intramembranous filaments composing the junctions were frequently reduced to single strands which

had a segmented and beaded appearance or showed short interruptions. Such patterns may represent disruptions of the junctions during fracture, with short segments or particles remaining associated with the E face, or reflect a process of remodeling (34). The permeability of the zonula occludens to lanthanum correlates well with the interrupted appearance of the junctions. Lanthanum has been shown to cross the tight junctions of natural leaky epithelia such as rabbit gallbladder and intestine (53) and rat proximal and distal convoluted tubules (57). It is therefore tempting to speculate that some of the discontinuities observed in the strands constitute channels where permeating substances cross the junction. Moreno and Diamond (62), who described Na^+-specific channels for the frog gallbladder, have suggested that this epithelium is traversed by Cl^- through leaks for free solution. The morphological appearance of a junction in freeze-fracture replicas, however, may not correlate well with its effectiveness as a barrier. Martinez-Palomo and Erlij (58) and Møllgard et al. (60) have shown that junctions with apparently similar organization may have electrical resistances orders of magnitude apart.

Several investigators (81, 58) have shown that hyperosmolarity, a treatment which reduces the resistance of an epithelium, opens tight junctions and increases the permeability to macromolecular tracers. It has recently been shown (39) that Ca^{++} removal may open tight junctions between glandular epithelial cells. We found that upon Ca^{++} removal and addition of EGTA, the electrical resistance of MDCK monolayers dropped sharply, while tight junctions and desmosomes were opened and intercellular gaps appeared at the level of the junctions between some of the cells. This observation suggests that Ca^{++} plays an important role as a bridging element between junctional components of neighboring cells. Freeze-fracture studies, to be described elsewhere, indicate that, immediately after Ca^{++} chelation, intramembranous strands are present although their network soon becomes disorganized and, finally, strands may be internalized. This supports the suggestion, from studies of pancreatic lobules incubated in Ca^{++}-free solutions containing EGTA (39), that Ca^{++} may also contribute to the organization and maintenance of the position of tight junctions in very specific regions of the cell.

We have shown that monolayers similar to those prepared with MDCK cells may be obtained with a variety of cell types. Thus, the technique described here may be applicable to many diverse areas of investigation where asymmetrical preparations with both surfaces accessible are required, and measurements without the contributions of connective tissue elements are desirable. An obvious advantage of tissue culture systems is that cells may be studied in the same medium in which they are cultured; therefore, artifacts and problems introduced by the shutoff of the blood supply when natural epithelia are mounted in chambers are avoided.

We are currently involved in a study of the development of functional polarization in the monolayers and are attempting to correlate the physiological properties with the acquisition of junctional complexes. The developing preparation is also well-suited to study the role of macromolecular synthesis and the effects of different inhibitors on the process of assembly of the junctions.[1]

We would like to thank Dr. Jorge Fischbarg of the Department of Ophthalmology, Columbia University for use of his equipment to measure water fluxes and helpful discussion, and Dr. William Crotty and the Biology Department of New York University Graduate School of Arts and Sciences for permission to use their evaporator and scanning electron microscope. In addition, we are pleased to acknowledge the hospitality and aid given by Dr. Dante Chiarandini, the able technical assistance of Dr. Monroe Yoder, Miss Heide Plesken, Mr. Miguel Nievas, and Mr. Fabian Cereijido, and the excellent secretarial assistance of Mrs. Myrna Cort. During part of these studies Marcelino Cereijido and Catalina A. Rotunno were fellows of the John Simon Guggenheim Memorial Foundation.

This work was supported with U. S. Public Health Service Research Grant AG00378.

A preliminary report of this work was presented in a symposium held at Yale University in June 1976, honoring the memory of Dr. Peter Curran (19). In addition, preliminary reports have been presented at several meetings (20, 21).

Received for publication 5 May 1977, and in revised form 10 February 1978.

REFERENCES

1. Abaza, N. A., J. Leighton, and S. G. Schultz. 1974. Effects of ouabain on the function and structure of a cell line (MDCK) derived from canine kidney. *In Vitro (Rockville).* **10:**172.
2. Barratt, L. J., F. C. Rector, J. P. Kokko, and D. W. Seldin. 1974. Factors governing the transepithelial potential difference across the proximal

tubule of the rat kidney. *J. Clin. Invest.* **53**:454.

3. BARRY, P. H., and J. M. DIAMOND. 1971. A theory of ion permeation through membranes with fixed neutral sites. *J. Membr. Biol.* **4**:295.
4. BARRY, P. H., J. M. DIAMOND, and E. M. WRIGHT. 1971. The mechanism of cation permeation in rabbit gallbladder. *J. Membr. Biol.* **4**:358.
5. BARRY, P. H., and A. B. HOPE. 1969. Electro-osmosis in membranes: effects of unstirred layers and transport numbers. II. Experimental. *Biophys. J.* **9**:729.
6. BELL, P. B., J. BRUNK, P. COLLINS, N. FORSBY, and B. A. FREDRIKSSON. 1975. SEM of cells in culture: osmotic effects during fixation. *In* Scanning Electron Microscope/1975 Proceedings of the 8th Annual Scanning Electron Microscope Symposium. Part I. O. Johari and I. Corvin, editors. ITT Research Institute, Chicago, Ill. 380.
7. BENTLEY, P. J. 1968. Amiloride: a potent inhibitor of sodium transport across the toad bladder. *J. Physiol. (Lond.).* **195**:317.
8. BORNSTEIN, M. B. 1973. Organotype Mammalian Central and Peripheral Nerve Tissue. *In* Tissue Culture. P. F. Kruse and M. K. Patterson, editors. Academic Press, Inc., New York. 86.
9. BOULPAEP, E. L. 1971. Electrophysiological properties of the proximal tubule: importance of cellular and intercellular transport pathways. *In* Electrophysiology of Epithelial Cells, G. Giebisch, editor. F.-K. Schattauer-Verlag, Stuttgart. 91.
10. BOULPAEP, E. L., and J. F. SEELY. 1971. Electrophysiology of proximal and distal tubules in the autoperfused dog kidney. *Am. J. Physiol.* **221**:1084.
11. BOURGUET, J., and S. JARD. 1964. Un dispositif automatique de mesure et d'en registrement du flux net d'eau a travers la peau et la vessie des amphibiens. *Biochim. Biophys. Acta.* **88**:442.
12. BRANTON, D., S. BULLIVANT, N. B. GILULA, M. J. KARNOVSKY, H. MOOR, K. MÜHLETHALER, D. H. NORTHCOTE, L. PACKER, B. SATIR, P. SATIR, V. SPETH, L. A. STAEHELIN, R. L. STEERE, and R. S. WEINSTEIN. 1975. Freeze-etching nomenclature. *Science (Wash. D.C.).* **190**:54.
13. BUENO, E. J., and L. CORCHS. 1968. Induced pacemaker activity on toad skin. *J. Gen. Physiol.* **51**:785.
14. CANDIA, O. A. 1970. The hyperpolarizing region of the current-voltage curve in frog skin. *Biophys. J.* **10**:323.
15. CASS, A., A. FINKELSTEIN, and V. KRESPI. 1970. The ion permeability induced in thin lipid membranes by the polyene antibiotics Nystatin and Amphotericin B. *J. Gen. Physiol.* **56**:100.
16. CEREIJIDO, M., and P. F. CURRAN. 1965. Intracellular electrical potentials in frog skin. *J. Gen. Physiol.* **48**:543.
17. CEREIJIDO, M., J. H. MORENO, E. RODRIGUEZ-BOULAN, and C. ROTUNNO. 1973. On the evaluation of fluxes across the outer border of the epithelium. *In* Role of Membranes in Secretory Processes. L. Bollis, editor. Elsevier North-Holland, Inc., New York. 279.
18. CEREIJIDO, M., C. RABITO, E. RODRIGUEZ-BOULAN, and C. A. ROTUNNO. 1974. The sodium transporting compartment of the epithelium of frog skin. *J. Physiol. (Lond.).* **237**:555.
19. CEREIJIDO, M., C. A. ROTUNNO, E. S. ROBBINS, and D. D. SABATINI. 1978. Polarized epithelial membranes produced *in vitro*. *In* Membrane Transport Processes. J. F. Hoffman, editor. Raven Press, New York. 433.
20. CEREIJIDO, M., C. A. ROTUNNO, E. S. ROBBINS, and D. D. SABATINI. 1977. In vitro formation of cell layers with properties of epithelial membranes. *Biophys. J.* **17**:229.
21. CEREIJIDO, M., E. S. ROBBINS, C. A. ROTUNNO, W. DOLAN, and D. D. SABATINI. 1977. Membrane properties of cells of renal origin (MDCK) cultured in monolayers on a permeable and translucent support. *Proc. Int. Union Physiol. Sci.* **12**:250.
22. CHEN, T. R. 1975. A simple rapid procedure to detect mycoplasma contamination in cell cultures. *Mammalian Chromosomes Newsletter.* **16**:137.
23. COHEN, A. L. 1974. Critical point drying. *In* Principles and Techniques of Scanning Electron Microscopy. A. M. Hayat, editor. Van Nostrand Reinhold Company, New York. 44.
24. CONTI, F., and G. EISENMAN. 1965. The steady-state properties of an ion exchange membrane with fixed sites. *Biophys. J.* **5**:511.
25. CONTI, F., and G. EISENMAN. 1966. The steady-state properties of an ion exchange membrane with mobile sites. *Biophys. J.* **6**:227.
26. CUTHBERT, A. W., and W. K. SHUM. 1974. Binding of Amiloride to sodium channels in frog skin. *Mol. Pharmacol.* **10**:880.
27. DIAMOND, J. 1962. Reabsorptive function of the gallbladder. *J. Physiol. (Lond.).* **161**:442.
28. DIPASQUALE, A., and P. B. BELL. 1974. The upper cell surface: its inability to support active cell movement in culture. *J. Cell Biol.* **62**:198.
29. DOBSON, J. G., and G. W. KIDDER. 1968. Edge damage effect: in vitro frog skin preparation. *Am. J. Physiol.* **214**:719.
30. DORGE, A., and W. NAGEL. 1970. Effect of Amiloride on sodium transport in frog skin. II. Sodium transport pool and unidirectional fluxes. *Pfluegers Arch. Eur. J. Physiol.* **321**:91.
31. EISENMAN, G. 1960. On the elementary atomic origin of equilibrium ionic specificity. *In* Symposium on Membrane Transport and Metabolism. A. Kleinzeller and A. Kotyk, editors. Academic Press, Inc. New York. 163.
32. EISENMAN, G. 1962. Cation selective glass electrodes and their mode of operation. *Biophys. J.* **2**(Pt. 2):259.
33. EISENMAN, G., J. P. SANDBOLM, and J. L.

WALKER. 1967. Membrane structure and ion permeation. *Science (Wash. D.C.)*. **155:**965.

34. ELIAS, P. M., and D. S. FRIEND. 1976. Vitamin-A-induced mucous metaplasia. An in vitro system for modulating tight and gap junction differentiation. *J. Cell Biol.* **68:**173.
35. FARQUHAR, M. G., and G. E. PALADE. 1963. Junctional complexes in various epithelia. *J. Cell Biol.* **17:**375.
36. FRIZZELL, R. A., and S. G. SCHULTZ. 1972. Ionic conductances of extracellular shunt pathway in rabbit ileum: influence of shunt on transmural sodium transport and electrical potential differences. *J. Gen. Physiol.* **59:**318.
37. FROMTER, E., and J. DIAMOND. 1972. Route of passive ion permeation in epithelia. *Nat. New Biol.* **235:**9.
38. FROMTER, E., C. W. MULLER, and T. WICK. 1971. Permeability properties of proximal tubular epithelium of the rat kidney studied with electrophysiological methods. *In* Electrophysiology of Epithelial Cells. F.-K. Schattauer-Verlag, Stuttgart. 119.
39. GALLI, P., A. BRENNA, P. DE CAMILLI, and J. MELDOLESI. 1976. Extracellular calcium and the organization of tight junctions in pancreatic acinar cells. *Exp. Cell Res.* **99:**178.
40. GOODENOUGH, D. A., and J. P. REVEL. 1970. A fine structural analysis of intercellular junctions in the mouse liver. *J. Cell Biol.* **45:**272.
41. HAGIWARA, S., R. GRUENER, H. HAYASHI, H. SAKATA, and A. D. GRINNEL. 1968. Effect of external and internal pH changes on K^+ and Cl^- conductances in muscle fiber membrane of a giant barnacle. *J. Gen. Physiol.* **52:**773.
42. HARRIS, J. B., and I. S. EDELMAN. 1964. Chemical concentration gradients and electrical properties of gastric mucosa. *Am. J. Physiol.* **206:**769.
43. HELMAN, S. I., J. J. GRANTHAM, and M. B. BURG. 1971. Effect of vasopressin on electrical resistance of renal cortical collecting tubules. *Am. J. Physiol.* **220:**1825.
44. HUDSPETH, A. J. 1975. Establishment of tight junctions between epithelial cells. *Proc. Natl. Acad. Sci. U.S.A.* **72:**2711.
45. HUTTER, O. F., and A. E. WARNER. 1967. The pH sensitivity of the chloride conductance of frog skeletal muscle. *J. Physiol. (Lond.)*. **189:**403.
46. KELLY, D. E., and F. L. SHIENVOLD. 1976. The desmosome: fine structural studies with freeze-fracture replication and tannic acid staining of sectioned epidermis. *Cell Tissue Res.* **172:**309.
47. KOEFOED-JOHNSON, V., and H. H. USSING. 1958. The nature of the frog skin potential. *Acta Physiol. Scand.* **42:**298.
48. KRAEHENBUHL, J. P., R. E. GALARDY, and J. D. JAMIESON. 1974. Preparation and characterization of an immunoelectron microscope tracer consisting of a heme-octapeptide coupled to Fab. *J. Exp. Med.* **139:**208.
49. LEB, D. E., T. HOSHIKO, and B. D. LINDLEY. 1965. Effects of alkali metal cations on the potential across toad and bullfrog urinary bladder. *J. Gen. Physiol.* **48:**527.
50. LEIGHTON, J., Z. BRADA, L. ESTES, and G. JUSTH. 1969. Secretory activity and oncogenicity of a cell line (MDCK) derived from canine kidney. *Science (Wash. D.C.)*. **163:**472.
51. LEIGHTON, J., L. W. ESTES, S. MANSUKHANI, and Z. BRADA. 1970. A cell line derived from normal dog kidney (MDCK) exhibiting qualities of papillary adenocarcinoma and of renal tubular epithelium. *Cancer (Phila.)* **26:**1022.
52. LING, G., and M. OCHSENFELD. 1966. Studies on ion accumulation in muscle cell. *J. Gen. Physiol.* **48:**819.
53. MACHEN, T. E., D. ERLIJ, and F. B. P. WOODING. 1972. Permeable junctional complexes. The movement of lanthanum across rabbit gallbladder and intestine. *J. Cell Biol.* **54:**302.
54. MADIN, S. H., and N. B. DARBY. 1958. As catalogued in: American Type Culture Collection catalog of strains **2:**47, 1975.
55. MAIZELS, M. 1968. Effect of sodium content on sodium efflux from human red cells suspended in sodium-free media containing potassium, rubidium, cesium or lithium chloride. *J. Physiol. (Lond.)*. **195:**657.
56. MALNIC, G., and G. GIEBISCH. 1972. Some electrical properties of distal tubular epithelium in the rat. *Am. J. Physiol.* **223:**797.
57. MARTINEZ-PALOMO, A., and D. ERLIJ. 1973. The distribution of lanthanum in tight junctions of the kidney tubule. *Pfluegers Arch. Eur. J. Physiol.* **343:**267.
58. MARTINEZ-PALOMO, A., and D. ERLIJ. 1975. Structure of tight junctions in epithelia with different permeability. *Proc. Natl. Acad. Sci. U.S.A.* **72:**4487.
59. MISFELDT, D. S., S. T. HAMAMOTO, and D. R. PITELKA. 1976. Transepithelial transport in cell culture. *Proc. Natl. Acad. Sci. U.S.A.* **73:**1212.
60. MØLLGARD, K., D. H. MALINOWSKA, and W. R. SAUNDERS. 1976. Lack of correlation between tight junction morphology and permeability properties in developing choroid plexus. *Nature (Lond.)*. **264:**293.
61. MORENO, J. H., and J. M. DIAMOND. 1974. Discrimination of monovalent inorganic cations by "tight" junctions of gallbladder epithelium. *J. Membr. Biol.* **15:**277.
62. MORENO, J. H., and J. M. DIAMOND. 1975. Cation permeation mechanisms and cation selectivity in "tight junctions" of gallbladder epithelium. *In* Membranes: A Series of Advances. G. Eisenman, editor. Marcel Dekker, Inc., New York. **3:**383.
63. POSTE, G., L. W. GREENHAM, L. MALLUCCI, P. REEVE, and D. J. ALEXANDER. 1973. The study of cellular "microexudates" by ellipsometry and their

relationship to the cell coat. *Exp. Cell Res.* **78:**303.
64. PRICAM, C., F. HUMBERT, A. PERRELET, and L. ORCI. 1974. A freeze-etch study of the tight junctions of the rat kidney tubules. *Lab. Invest.* **30:**286.
65. RAU, W. S., and E. FROMTER. 1974. Electrical properties of the medullary collecting ducts of the golden hamster kidney. *Pfluegers Arch. Eur. J. Physiol.* **351:**113.
66. REVEL, J. P., and M. J. KARNOVSKY. 1967. Hexagonal array of subunits in intercellular junctions of the mouse heart and liver. *J. Cell Biol.* **33:**C7.
67. ROBINSON, R. A., and R. M. STOKES. 1970. Electrolyte solutions. Butterworth & Co. Ltd., London.
68. SABATINI, D. D., K. BENSCH, and R. BARRNETT. 1963. Cytochemistry and electronmicroscopy. The preservation of cellular ultrastructure and enzymatic activity by aldehyde fixation. *J. Cell Biol.* **17:**19.
69. SALAKO, L. A., and A. J. SMITH. 1970. Changes in sodium pool and kinetics of sodium transport in frog skin produced by Amiloride. *Br. J. Pharmacol.* **39:**99.
70. SCHULTZ, S., P. CURRAN, and E. WRIGHT. 1967. Interpretation of hexose-dependent electrical potential differences in small intestine. *Nature (Lond.).* **214:**509.
71. SCHULTZ, S. G., R. A. FRIZZEL, and H. N. NELLANS. 1974. Ion transport by mammalian small intestine. *Annu. Rev. Physiol.* **36:**51.
72. SCHULTZ, S., and R. ZALUSKY. 1963. The interaction between active sodium transport and active sugar transport in the isolated rabbit ileum. *Biochim. Biophys. Acta.* **71:**503.
73. SHIMONO, M., and F. CLEMENTI. 1976. Intercellular junctions of oral epithelium. I. Studies with freeze-fracture and tracing methods in normal rat keratinized epithelium. *J. Ultrastruct. Res.* **56:**121.
74. SJODIN, R. A., and L. A. BEAUGE. 1968. Coupling and selectivity of sodium and potassium transport in squid giant axons. *J. Gen. Physiol.* **51**(Pt. 2)**:**152.
75. SMULDERS, A. P., TORMEY, J. McD., and E. M. WRIGHT. 1972. The effect of osmotically induced water flow on the permeability and ultrastructure of the rabbit gallbladder. *J. Membr. Biol.* **7:**164.
76. SPRING, K. R., and C. V. PAGANELLI. 1972. Sodium flux in *Necturus* proximal tubule under voltage clamp. *J. Gen. Physiol.* **60:**181.
77. STOKER, M. G. P. 1973. Role of diffusion boundary layer in contact inhibition of growth. *Nature (Lond.).* **246:**200.
78. TEORELL, T. 1953. Transport processes and electrical phenomena in ionic membranes. *In* Progress in Biophysics and Biophysical Chemistry. J. A. V. Butler and J. T. Randall, editors. Pergamon Press Ltd., Oxford. **3:**305.
79. TODARO, G. J., G. K. LAZAR, and H. GREEN. 1965. The initiation of cell division in a contact-inhibited mammalian cell line. *J. Cell. Comp. Physiol.* **66:**325.
80. USSING, H. H. 1952. Some aspects of the application of tracers in permeability studies. *Adv. Enzymol. Relat. Areas Mol. Biol.* **13:**21.
81. USSING, H. H., and E. E. WINDHAGER. 1964. Nature of shunt path and active Na^+ transport path through frog skin epithelium. *Acta Physiol. Scand.* **61:**484.
82. WEDNER, H. J., and J. DIAMOND. 1969. Contributions of unstirred-layer effects to apparent electrokinetic phenomena in the gallbladder. *J. Membr. Biol.* **1:**92.
83. WIEDNER, G., and E. M. WRIGHT. 1975. The role of lateral intercellular spaces in the control of ion permeation across the rabbit gallbladder. *Pfluegers Arch. Eur. J. Physiol.* **358:**27.
84. WHITTEMBURY, G., and F. A. RAWLINS. 1971. Evidence of a paracellular pathway for ion flow in the kidney proximal tubule: electron microscopic demonstration of lanthanum precipitate in the tight junction. *Pfluegers Arch. Eur. J. Physiol.* **330:**302.
85. WRIGHT, E. M. 1970. Ion transport across the frog choroid plexus. *Brain Res.* **23:**302.
86. WRIGHT, E. M. 1972. Mechanism of ion transport across the choroid plexus. *J. Physiol. (Lond.).* **226:**545.
87. WRIGHT, E. M., P. H. BARRY, and J. DIAMOND. 1971. The mechanism of cation permeation in rabbit gallbladder. *J. Membr. Biol.* **4:**331.
88. WRIGHT, E. M., and J. M. DIAMOND. 1968. Effect of pH and polyvalent cations on the selective permeability of gallbladder epithelium to monovalent ions. *Biochim. Biophys. Acta.* **163:**57.